European Journal of Taxonomy 19: 1-34
http://dx.doi.org/10.5852/ejt.2012.19

ISSN 2118-9773
www.europeanjournaloftaxonomy.eu
2012 · M.B. Forel

Research article

Ostracods (Crustacea) associated with microbialites across the Permian-Triassic boundary in Dajiang (Guizhou Province, South China)

Marie-Béatrice FOREL

State Key Laboratory of Geological Process and Mineral Resources, China University of Geosciences, No. 388, Lumo Road, Wuhan 430074, People's Republic of China.
E-mail: mbforel@yahoo.fr

Abstract. 26 samples were processed for a taxonomic study of ostracods from the Upper Permian (Changhsingian) - Lower Triassic (Griesbachian) interval of the Dajiang section, Guizhou Province, South China. 112 species belonging to 27 genera are recognized. Five new species are described: *Acratia candyae* sp. nov, *Bairdia adelineae* sp. nov., *Bairdia*? *huberti* sp. nov., *Bairdia jeromei* sp. nov., *Orthobairdia jeanlouisi* sp. nov. The unexpected survival faunas associated with microbial formations in the aftermath of the end-Permian extinction are documented for the first time. Ostracod biodiversity variations and palaeo-environmental modifications associated with microbial growth through the Permian-Triassic boundary (PTB) are discussed.

Keywords. Ostracods, Permian-Triassic, Microbialites, Dajiang, South China.

Forel M.B. 2012. Ostracods (Crustacea) associated with microbialites across the Permian-Triassic boundary in Dajiang (Guizhou Province, South China). *European Journal of Taxonomy* 18: 1-34. http://dx.doi.org/10.5852/ejt.2012.19

Introduction

The end-Permian extinction, about 252 My, decimated 80 to 96% of species and 52% of families in the marine realm (e.g. Sepkoski 1984; Erwin 1993; Benton & Twitchett 2003). Several potential geological triggers have been identified: bolide impact, oceanic anoxia and euxinia and flood basalt volcanism. It is now accepted that ocean anoxia was widespread during the latest Permian (Changhsingian), its prevalence increased near the time of the main extinction and continued during the Early Triassic. Anoxic and sulfidic waters commonly also extended into shallow-marine environments. The eruption of the Siberian Traps is now considered as the primary trigger of extinction. Global warming, ocean acidification, and possible destruction of atmospheric ozone were engendered by the release of volcanic CO_2 and volatilized sedimentary organic carbon and evaporite minerals. Enhanced weathering and nutrient runoff increased pre-existing ocean anoxia (see Payne & Clapham 2012 and references therein for details). The extinction marks a major transition in marine ecosystems: the Upper Permian benthic shelly communities from shallow marine settings were replaced by widespread microbial communities. They are abundant in low-latitude shallow-marine carbonate shelves in central Tethyan continents where they occupied similar environments to Upper Permian reefs but extended into deeper waters

Fig. 1. Location of the Dajiang section in the southern Guizhou Province, South China.

(Kershaw *et al.* 2007, 2012). Current evidence regarding oxygen levels associated with microbialites growth is conflicting : (*i*) evidence of low-oxygen conditions (Bond & Wignall 2010; Liao *et al.* 2010; Chen *et al.* 2011), (*ii*) abundant benthic shelly faunas dominated by ostracods, and occasionally some rare micro-gastropods, microbrachiopods, foraminifers and conodonts (e.g. Crasquin-Soleau & Kershaw 2005; Forel *et al.* 2009; Song *et al.* 2009; Yang *et al.* 2011; Forel *et al.* in press). A two-steps oxygenation of the surrounding waters by cyanobacterial activity will be proposed as a possible mechanism for this unexpected survival (Forel in press).

74 to 100% of ostracods became extinct through the Permian-Triassic boundary (PTB) and very little is known about their presence and characteristics in the interval following the extinction event. In the lower Griesbachian neritic environments, they are only found in association with microbialites. The faunas described in the present article are of primary importance because they exemplify a survival phenomenon in a refuge of microbial origin documented from several localities worldwide (Forel in press; Forel *et al.* in press). This paper describes the upper Changhsingian and lower Griesbachian ostracod faunas of the Dajiang section (Wujiaping and Daye Formations respectively), Guizhou Province, South China. 112 species are recorded, including 5 new species, belonging to 27 genera.

Material and Methods

The Dajiang section (25°33'56''N-106°39'41''E) is located in the southern Guizhou Province, South China, a few kilometres north of the city of Luodian (Fig. 1). Only a brief description of the lithological succession in Dajiang is given here: the reader is referred to Forel *et al.* (2009) and references therein for further details. At the base of the section are about 7 metres of open shallow marine thick, massive-bedded skeletal lime-packstone of the Wujiaping Formation (Changhsingian age). They are followed by about 17 metres of microbialite carbonate layers of the Daye Formation. The conodont *Hindeodus parvus* (Kozur & Pjatakova, 1976) occurs throughout the lowermost metre-thick microbialite carbonate, above the major facies change that marks the greatest loss in Permian fossils (the first occurrence of *H. parvus* is the index of the base of the Triassic: Yin *et al.* 1996; Lehrmann 1999; Lehrmann *et al.* 2003). The PTB 'event horizon' corresponds to the contact between the Wujiaping Formation and the microbialite (Lehrmann *et al.* 2003).

Samples spanning the Permian-Triassic event horizon were collected for ostracod analysis and labelled as 05PAJxx (Fig. 2). Ostracods are determined on the basis of external and internal characters of the carapace and have to be released from the enclosing matrix. Extraction by means of acid is precluded because their carapaces are made of calcium carbonate and enclosed in calcareous rocks. Samples were processed by hot acetolysis technique to disaggregate the dehydrated hard limestones and release the ostracod shells (Lethiers & Crasquin-Soleau 1988; Crasquin-Soleau *et al.* 2005). Twenty-six samples were collected and analysed, only one was barren (05PAJ34; Fig. 2). The faunas in Dajiang show high intraspecific variability that hindered the clear differentiation between species in many cases. Due to the poor preservation and availability of specimens, many species are left in open nomenclature and are not listed in the systematic part (e.g. *Bairdia* sp. 1 to 36), although all the material of this important interval is figured. All specimens are stored in the Pierre et Marie Curie University Collections (Paris, France; collection numbers P6M2917-3150).

All the species belonging to the Bairdioidea (Sars, 1887) superfamily are shown in Figs 3 (genera *Acratia* Delo, 1930 and *Bairdia* McCoy, 1844), 4, 7-9 (genus *Bairdia*), 10 (genera *Bairdia* and *Bairdiacypris* Bradfield, 1935), 11 (genera *Bairdiacypris*, *Bythocypris* Brady, 1880, *Fabalicypris* Brady, 1880, *Liuzhinia* Zheng, 1976 and *Orthobairdia* Sohn, 1960) and 13 (genera *Petasobairdia* Chen, 1982, *Spinocypris* Kozur, 1971, *Kempfina* Crasquin, 2010, *Silenites* Coryell & Booth, 1933 and *Microcheilinella* Geis, 1933). Species belonging to the Cypridoidea Baird, 1845 are gathered in Figs 13 and 14 (genus *Paracypris* Sars, 1866). Cytheroidea Baird, 1850 are shown in Figs 14 (genera *Monoceratina*

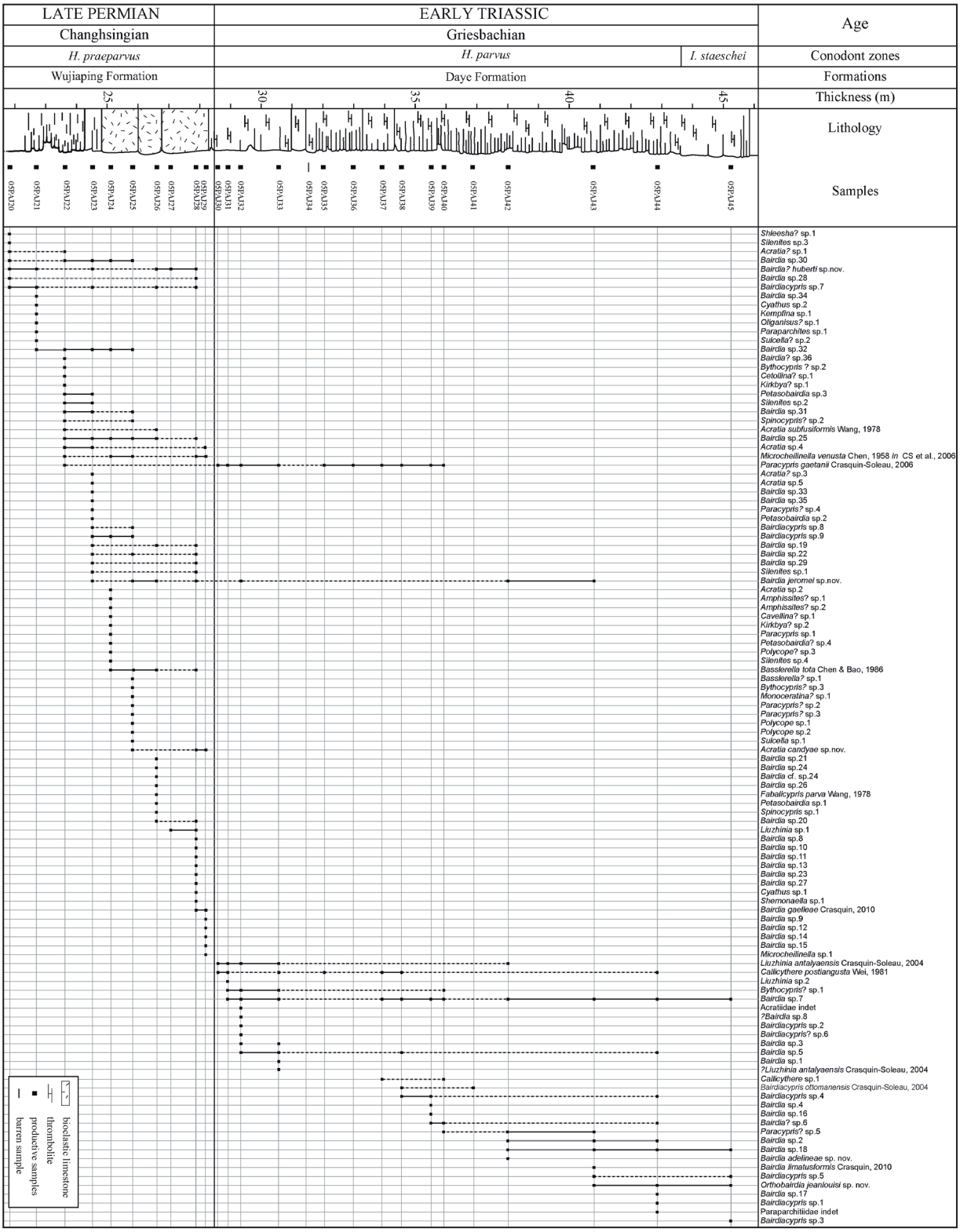

Fig. 2. Lithostratigraphy of the Dajiang Section, with the location of studied samples and ostracod species distribution through the section.

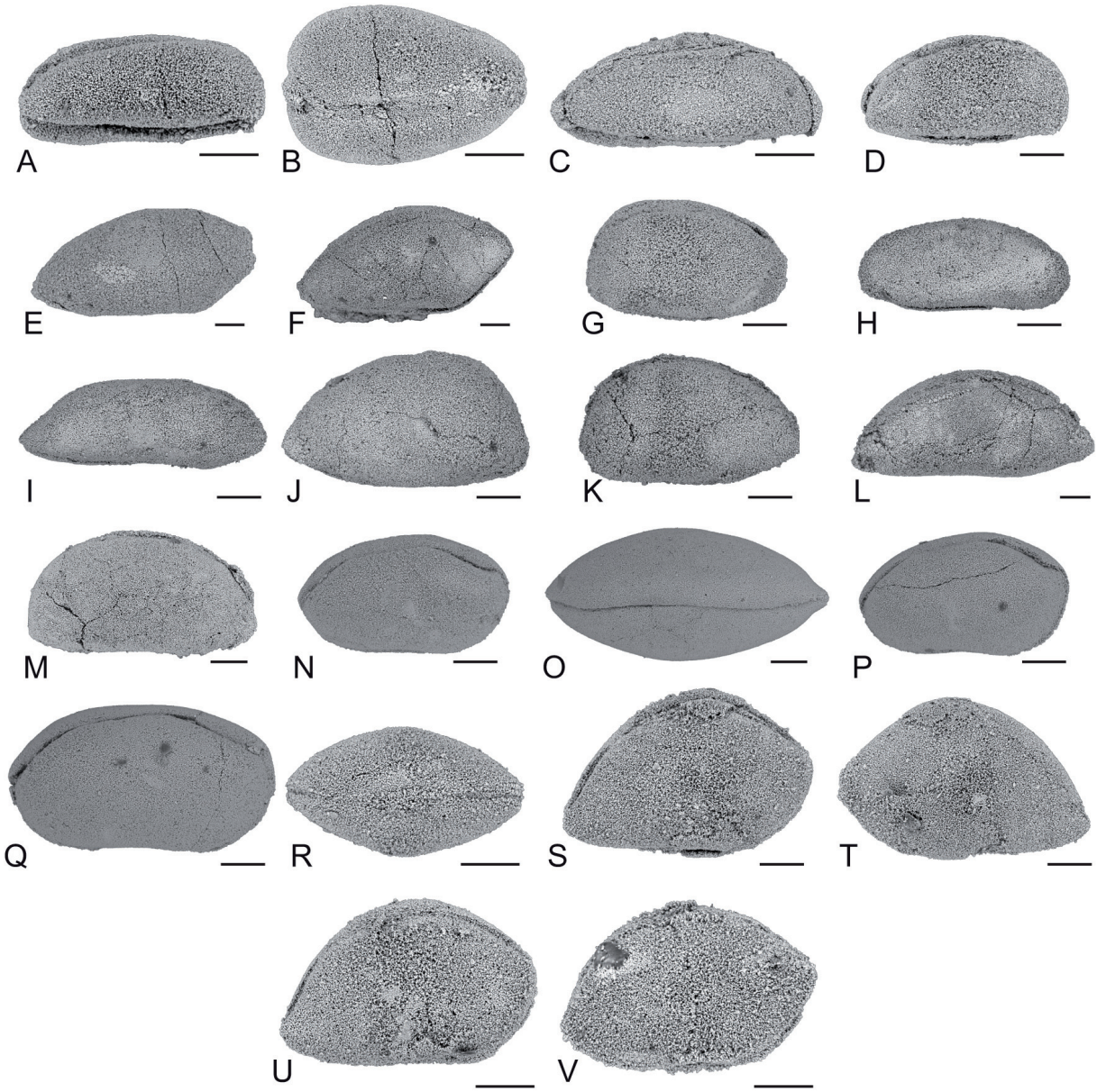

Fig. 3. Ostracods from the Dajiang section, South China. — **A–D**. *Acratia candyae* sp. nov. **A**. Holotype, carapace, right lateral view, P6M2917. **B**. Carapace, dorsal view, P6M2918. **C**. Paratype, carapace, right lateral view, P6M2919. **D**. Carapace, right lateral view, P6M2920. — **E–F**. *Acratia subfusiformis* Wang, 1978. **E**. Carapace, right lateral view, P6M2921. **F**. Carapace, right lateral view, P6M2922. — **G**. *Acratia*? sp. 1, carapace, right lateral view, P6M2923. — **H**. *Acratia*? sp. 2, carapace, right lateral view, P6M2924. — **I**. *Acratia*? sp. 3, carapace, right lateral view, P6M2925. — **J–K**. *Acratia* sp. 4. **J**. Carapace, left lateral view, P6M2926. **K**. Carapace, right lateral view, P6M2927. — **L**. *Acratia* sp. 5, carapace, right lateral view, P6M2928. — **M**. Acratiidae indet., carapace, right lateral view, P6M2929. — **N–Q**. *Bairdia adelineae* sp. nov. **N**. Holotype, carapace, right lateral view, P6M2930. **O**. Carapace, dorsal view, P6M2931. **P**. paratype, carapace, right lateral view, P6M2932. **Q**. Carapace, right lateral view, P6M2933. — **R–V**. *Bairdia gaelleae* Crasquin, 2010. **R**. Carapace, dorsal view, P6M2934. **S**. Carapace, right lateral view, P6M2935. **T**. Carapace, left lateral view, P6M2936. **U**. Carapace, right lateral view, P6M2937. **V**. Carapace, right lateral view, P6M2938. – Scale = 100 µm.

Roth, 1928, *Basslerella* Kellett, 1935 and *Callicythere* Wei, 1981) and 15 (genus *Callicythere*). Cavellinidae Egorov, 1950 (genus *Sulcella* Coryell & Sample, 1932), Polycopidae Sars, 1866 (genus *Polycope* Sars, 1866), Aparchitidae Jones, 1901 (genus *Cyathus* Roth & Skinner, 1930), Kirkbyoidea Ulrich & Bassler, 1906 (genera *Amphissites* Girty, 1910, *Kirkbya* Jones, 1859 and *Shleesha* Sohn, 1961), Kloedenellidae Ulirch & Bassler, 1908 (genus *Oliganisus* Geis, 1932) and Paraparchitidae Scott, 1959 (genera *Paraparchites* Ulrich & Bassler, 1906 and *Shemonaella* Sohn, 1971) are shown in Fig. 15.

Abbreviations used in the text

RV = right valve
LV = left valve
AB = anterior border
PB = posterior border
DB = dorsal border
VB = ventral border
ADB = antero-dorsal border
AVB = antero-ventral border
PDB = postero-dorsal border
PVB = postero-ventral border
H = height
Hmax = maximal height
L = length
Lmax = maximal length
W = width
Wmax = maximal width

Results

Taxonomic descriptions

Class Ostracoda Latreille, 1802
Order Podocopida Müller, 1894
Sub-order Podocopina Sars, 1866
Superfamily Bairdioidea Sars, 1888
Family Acratiidae Gründel, 1962
Genus *Acratia* Delo, 1930

Acratia candyae sp. nov.
Fig. 3A-D

Diagnosis

Species of *Acratia* similar to *Microcheilinella* in dorsal view, with LV larger than RV and AB broadly rounded in 1/4 circle.

Etymology

Personal dedication to Candy Boiteux.

Material examined

Holotype

One carapace (Fig. 3A), Dajiang section, sample 05PAJ28, collection number P6M2917.

Paratype

One carapace (Fig. 3C), Dajiang section, sample 05PAJ17, collection number P6M2919.

Other material

4 carapaces, several fragments. The species is known from its type locality only.

Type locality

Wujiaping Formation (Samples 05PAJ17, 25, 28, 29), Dajiang section (25°33'56''N-106°39'41''E), Guizhou Province, South China, Changhsingian, Late Permian.

Measurements

L = 323 – 464 μm; H = 140 – 200 μm; H/L = 0.43 – 0.44.

Description

Carapace elongated and subovoid in lateral view; surface smooth; carapace slightly preplete to amplete; LV strongly overlaps RV all around the carapace; Lmax below mid-H; dorsum long and slightly rounded in both valves, angles between PDB and DB not distinct; rounded angle between DB and ADB (~140°); PDB short and steep; DB long and gently bent backward; ADB short, steep and convex; ventral margin flat and straight at both valves; AVB, VB, PVB not distinct; AVB straight and slightly bent toward AB; AB broadly rounded in 1/4 circle; acratian beak clear but not pronounced, located at VB; PB sharpen with quite large radius of curvature for the genus, maximum slightly below mid-H; angle between AVB-AB (>90°) larger than angle between PVB-PB (<90°); dorsal view similar to the one of the genus *Microcheilinella* with carapace thick and Wmax located in the posterior 1/3 of L, hinge line slightly incised.

Through the ontogeny, the carapace becomes more stocky, more amplete at RV, with DB shorter and more rounded.

Remarks

The strong overlap of LV on RV all around the carapace and characteristics of dorsal view are reminiscent of the genus *Microcheilinella*. However the acratian beak clearly precludes *Microcheilinella* attribution and indicates the genus *Acratia*. *Acratia candyae* sp. nov. is very close to *Acratia* sp.2 *sensu* Crasquin, 2008 from the Late Permian of Dolomites (Crasquin *et al.* 2008). However, *Acratia* sp.2 *sensu* Crasquin, 2008 has longer ADB and well expressed angles between PDB, DB and ADB.

Acratia subfusiformis Wang, 1978
Figs 3E-F

Acratia subfusiformis Wang, 1978: 294-295, pl.4, figs 3-4.

Acratia subfusiformis – Shi & Chen 1987: 49, pl.11, figs 19-22, pl. 12, figs 1-2 — Shi & Chen 2002: 82, pl.20, figs 1-9. — Crasquin *et al.* 2010: 357, figs 23I-L.
? *Acratia subfusiformis* – Shi & Chen 2002: 82, pl. 20, figs 12-13.
Not *Acratia subfusiformis* – Shi & Chen 2002: 82, pl. 20, figs 10-11.

Localities

- Wujiaping Formation (samples 05PAJ22, 26), Dajiang section (25°33'56''N-106°39'41''E), Guizhou Province, South China, Changhsingian, Late Permian.
- Longtan Formation, Northern Guizhou and Southern Yunnan Provinces, South China, Wuchiapingian, Late Permian (Wang 1978).

- Baoqing Member, Changxing Formation, Meishan section, Zhejiang Province, South China, Changhsingian, Late Permian (Shi & Chen 1987).
- Matan and Pingding sections, Guangxi Province, South China Wuchiapingian and Changhsingian, Late Permian (Shi & Chen 2002).
- Baoqing and Meishan Members, Changxing Formation, Meishan section, Zhejiang Province, South China, Changhsingian, Late Permian (Crasquin *et al.* 2010).

Family Bairdiidae Sars, 1887
Genus *Bairdia* McCoy, 1844

Bairdia adelineae sp. nov.
Fig. 3N-Q

Diagnosis

Stocky species of *Bairdia* with strong dorsal overlap, laterally flattened plateau-like DB, AB and PB with large radius of curvature.

Etymology

Personal dedication to Adeline Bienvenu.

Material examined

Holotype

One carapace (Fig. 3N), sample 05PAJ42, collection number P6M2930.

Paratype

One carapace (Fig. 3P), sample 05PAJ42, collection number P6M2932.

Other material

4 carapaces, several fragments. The species is known from its type locality only.

Type locality

Daye Formation (Sample 05PAJ42), Dajiang section (25°33'56''N-106°39'41''E), Guizhou Province, South China, Griesbachian, Early Triassic.

Measurements

L = 513 – 655 μm; H = 292 – 347 μm; H/L = 0.53 – 0.58.

Description

Carapace elongated and massive, subovoid in lateral view; surface smooth; carapace amplete to preplete; LV overlapping RV all around the carapace, dorsal overlap stronger than ventral one; dorsum subdivided into 3 distinct parts at both valves; PDB straight to slightly convex; DB straight at both valves, flattened laterally at RV; ADB straight to slightly concave at anterior extremity; DB and ADB longer than PDB; VB long and slightly concave in median part at RV, straight to slightly concave at LV; AVB broadly rounded and long (~ 75% of Hmax); PVB straight to convex and short (<50% of Hmax); AB rounded with large radius of curvature, maximum in the upper 1/3 of H, bairdian beak poorly expressed but distinct; PB pointed with large radius of curvature, maximum at or slightly below mid-H; in dorsal view, carapace lenticular and thick with anterior extremity slightly tapered, Wmax located around mid-L, plateau-like laterally flattened at RV.

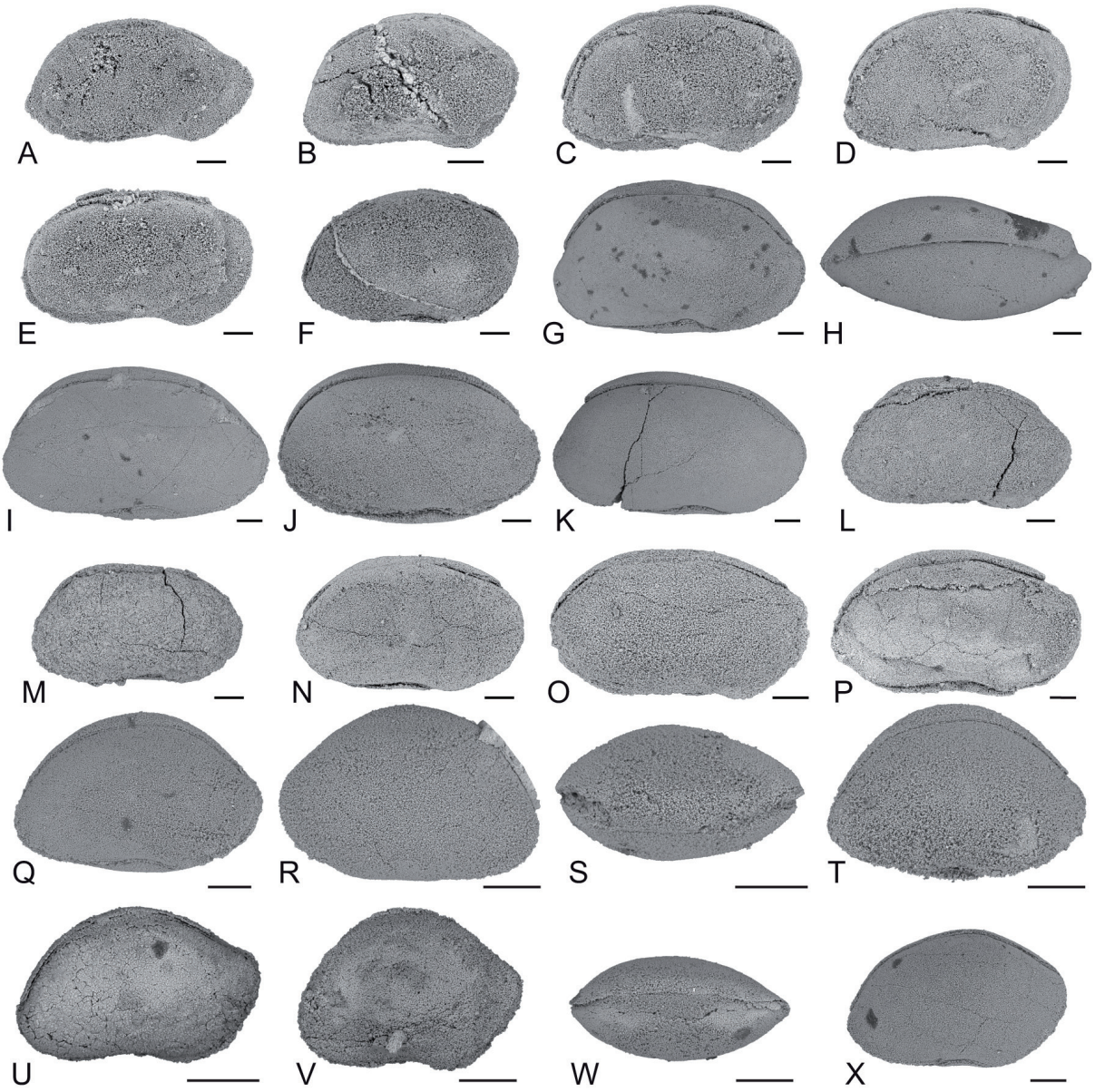

Fig. 4. Ostracods from the Dajiang section, South China. — **A–F**. *Bairdia*? *huberti* sp. nov. **A**. Carapace, right lateral view, P6M2939. **B**. Carapace, right lateral view, P6M2940. **C**. Paratype, carapace, right lateral view, P6M2941. **D**. Holotype, carapace, right lateral view, P6M2942. **E**. Carapace, right lateral view, P6M2943. **F**. Carapace, right lateral view, P6M2944. — **G–P**. *Bairdia jeromei* sp. nov. **G**. Holotype, carapace, right lateral view, P6M2945. **H**. Carapace, dorsal view, P6M2946. **I**. Carapace, right lateral view, P6M2947. **J**. Paratype, carapace, right lateral view, P6M2948. **K**. Carapace, right lateral view, P6M2949. **L**. Carapace, right lateral view, P6M2950. **M**. Carapace, right lateral view, P6M2951. **N**. Carapace, right lateral view, P6M2952. **O**. Carapace, right lateral view, P6M2953. **P**. Carapace, right lateral view, P6M2954. — **Q–T**. *Bairdia limatusformis* Forel, 2010. **Q**. Carapace, right lateral view, P6M2955. **R**. Carapace, left lateral view, P6M2956. **S**. Carapace, sub-dorsal view, P6M2957. **T**. Carapace, right lateral view, P6M2958. — **U–V**. *Bairdia* sp. 1. **U**. Carapace, right lateral view, P6M2959. **V**. Carapace, right lateral view, P6M2960. — **W–X**. *Bairdia* sp. 2. **W**. Carapace, dorsal view, P6M2961. **X**. Carapace, right lateral view, P6M2962. – Scale = 100 µm.

Remarks

This new species can be related to *Bairdia paussi* Crasquin, 2010 from the Late Permian of the Meishan section, Zhejiang Province, South China (Crasquin *et al.* 2010). However *Bairdia adelineae* sp. nov. is more elongated, with stronger overlap and posterior maximum of convexity located closer to VB. It can also be compared to *Orthobairdia texana* (Harlton, 1927) *sensu* Shi & Chen, 2002 from the Permian of Heshan and Yishan, Guangxi Province, South China (Shi & Chen 2002). However, the bairdioid dorsal view precludes generic attribution to *Orthobairdia*. *Bairdia adelineae* sp.nov is also close to *Bairdia chasae* Kellett, 1934 *sensu* Wang, 1978 from the Late Permian of the Western Guizhou and Northeastern Yunnan Provinces, South China (Wang 1978). However the new species has a less pointed PB, a thinner ventral overlap and the dorsal view clearly shows a bairdioid shape. It is noteworthy that *Bairdia chasae* Kellett, 1935 *sensu* Wang, 1978 seems wrongly attributed to the genus *Bairdia*: the dorsal view shows a typical orthobairdian shape.

Bairdia gaelleae Crasquin, 2010
Fig. 3R-V

Bairdia gaelleae Crasquin, 2010: 344-346, figs 13W-Z.

? *Bairdia hassi* – Shi & Chen 2002: 66, pl. 4, figs 11–15.

Localities

- Wujiaping Formation (samples 05PAJ, 28, 29), Dajiang section (N25°33'56''-E106°39'41''), Guizhou Province, South China, Changhsingian, Late Permian.
- Matan and Pingding sections, Guangxi Province, South China, Wuchiapingian, Late Permian (Shi & Chen 2002).
- Baoqing and Meishan members, Changxing Formation, Meishan section, Zhejiang Province, South China, Changhsingian, Late Permian (Crasquin *et al.* 2010).

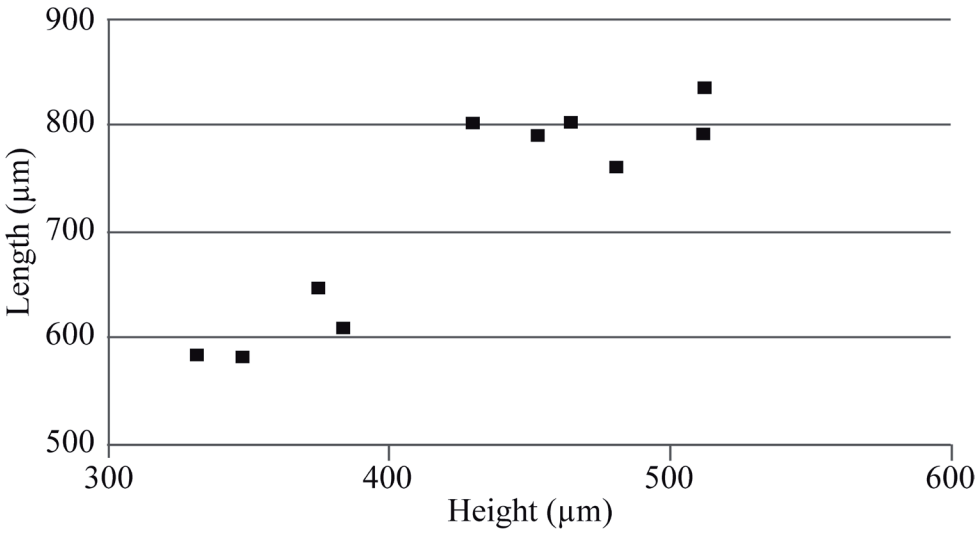

Fig. 5. Height/length diagram of *Bairdia* ?*huberti* sp. nov.

Bairdia*? *huberti sp. nov.
Fig. 4A-F

Diagnosis

Species attributed with doubt to the genus *Bairdia*, with relatively elongated carapace, ADB and DB not distinct, very large AB.

Etymology

Personal dedication to Hubert Colas.

Material examined

Holotype

One carapace (Fig. 4D), sample 05PAJ28, collection number P6M2942.

Paratype

One carapace (Fig. 4C), sample 05PAJ28, collection number P6M2941.

Other material

10 carapaces, several fragments. The species is known from its type locality only.

Type locality

Wujiaping Formation (samples 05PAJ20, 21, 23, 26-28), Dajiang section (25°33'56''N-106°39'41''E), Guizhou Province, South China, Changhsingian, Late Permian.

Measurements (Fig. 5)

L = 581 – 837 μm; H = 332 – 512 μm; H/L = 0.53 – 0.64.

Description

Carapace relatively elongated, ovoid in lateral view; PDB long, straight to slightly convex; PDB-DB angle around 110°; DB and ADB not clearly distinct and along relative constant H, close to Hmax; VB concave; AVB rounded and long (~ 75% of Hmax); PVB very short and rounded; AB with large radius of curvature, maximum located on the upper 1/4 of H; PB with narrow radius of curvature, maximum located in the lower 1/4 of H; Lmax located around mid-H.

Remarks

High intraspecific variations that mainly affect the ADB and AB are observed in *Bairdia*? *huberti* sp. nov. They create continuum between *Cryptobairdia*-like (ABD not distinct: Fig. 4C-E) and *Bairdia*-like specimens (ABD differentiated: Fig. 4A, B, F). The new species is therefore attributed with doubt to the genus *Bairdia*. *Bairdia*? *huberti* sp. nov. is similar to *Bairdia broutini* Crasquin, 2010 from the Late Permian of the Meishan section, Zhejiang Province, South China (Crasquin *et al.* 2010) because of the relative constant and high H. However, the new species is more elongated, with longer DB.

Bairdia jeromei sp. nov.
Fig. 4G-P

Diagnosis

Massive and subrectangular species of *Bairdia*, with DB and VB subparallel, long DB (~ 60% of Lmax), rhombic dorsal view.

Etymology

Personal dedication to Jérôme Cougoul.

Material examined

Holotype

One carapace (Fig. 4G), sample 05PAJ43, collection number P6M2945.

Paratype

One carapace (Fig. 4J), sample 05PAJ43, collection number P6M2948.

Other material

10 carapaces, several fragments. The species is known from its type locality only.

Type locality

Wujiaping and Daye Formations (samples 05PAJ23, 25, 26, 28, 32, 42, 43), Dajiang section (25°33'56''N-106°39'41''E), Guizhou Province, South China, Changhsingian and Griesbachian, Late Permian and Early Triassic.

Measurements (Fig. 6)

L = 722 – 1024 µm; H = 410 – 597 µm; H/L = 0.56 – 0.64.

Description

Carapace massive, elongated and subrectangular in lateral view; surface smooth; LV larger than RV, overlapping at dorsum and VB; bairdian beaks at AB and PB poorly expressed; PDB, DB and ADB distinct at both valves; PDB steeply bent backward, long (~ 65% of Hmax) and slightly convex; DB long (~60% of Lmax) and gently convex; ADB slightly concave at RV, shorter than PDB; ventral

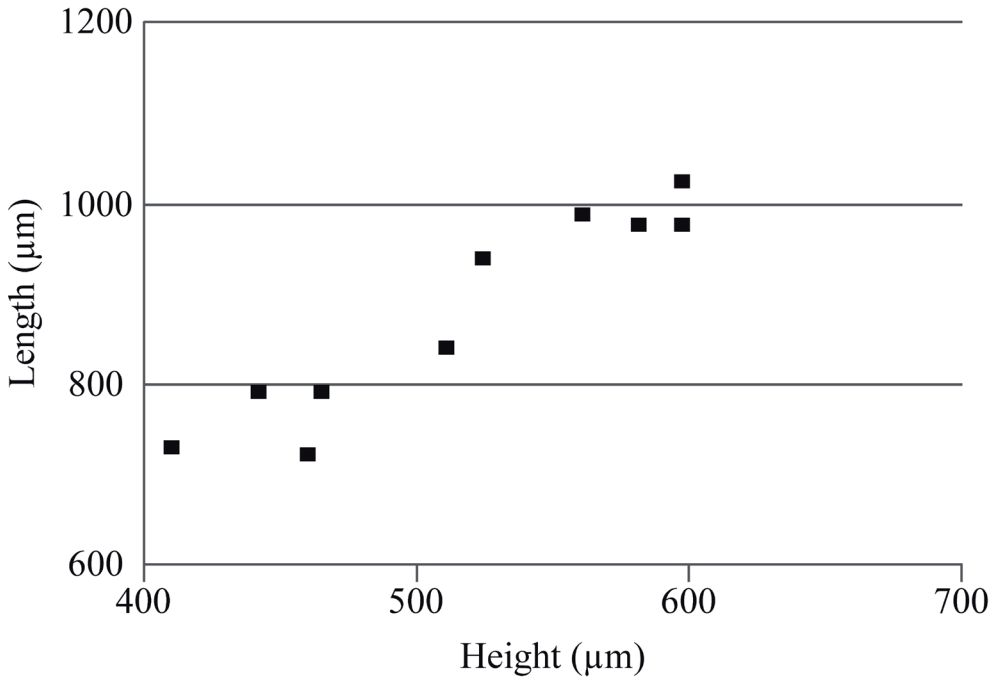

Fig. 6. Height/length diagram of *Bairdia jeromei* sp. nov.

part rounded; VB long, convex at LV, concave at RV; AVB and PVB rounded, AVB longer than PVB; carapace slightly postplete to amplete; Lmax below mid-H; dorsal view rhombic with LV's Wmax in posterior 1/3 of Lmax, in anterior 1/3 at RV.

Remarks

In lateral view, *Bairdia jeromei* sp. nov. is similar to *Orthobairdia* sp.1 *sensu* Crasquin *et al.*, 2010 from the Permian of the Meishan section, Zhejiang Province, South China (Crasquin *et al.* 2010) but here the dorsal view clearly precludes the generic attribution to *Orthobairdia*.

Bairdia limatusformis Forel, 2010
Fig. 4Q-T

Silenites limatus – Shi & Chen 1987: 62, pl.15, figs 15-19.
Bairdia limatusformis – Crasquin *et al.* 2010: 346-347, figs 9E-G.
Not *Silenites limatus* – Shi & Chen 2002: 95, pl.27, figs 2-17.

Localities

- Daye Formation (sample 05PAJ43), Dajiang section (25°33'56''N-106°39'41''E), Guizhou Province, South China, Griesbachian, Early Triassic.
- Baoqing and Meishan members, Changxing formation, Meishan section, Zhejiang Province, South China, Changhsingian, Late Permian (Shi & Chen 1987; Crasquin *et al.* 2010).
- Matan and Pingding sections, Guangxi Province, South China, Wuchiapingian, Late Permian (Shi & Chen 2002).

Genus *Bairdiacypris* Bradfield, 1935

Bairdiacypris ottomanensis Crasquin-Soleau, 2004
Fig. 10E-H

Bairdiacypris ottomanensis Crasquin-Soleau, 2004: 285-286, pl. 2, figs 13-24.

Bairdiacypris ottomanensis – Crasquin-Soleau & Kershaw 2005: pl. I, figs 10-12. — Forel *et al.* 2009: 819, fig. 4 (1).

Localities

- Daye Formation (samples 05PAJ38, 41), Dajiang section (25°33'56''N-106°39'41''E), Guizhou Province, South China, Griesbachian, Early Triassic (Forel *et al.* 2009; this study).
- Kokarkuyu Formation, Çürük dağ section, Western Taurus, Antalya Nappes, Turkey, Early Triassic (Crasquin-Soleau *et al.* 2004).
- Feixianguan Formation, Laolongdong section, Sichuan Province, South China, Induan, Early Triassic (Crasquin & Kershaw 2005).

Genus *Fabalicypris* Brady, 1880

Fabalicypris parva Wang, 1978
Fig. 11I

Fabalicypris parva Wang, 1978: 293, pl. 2, figs 12a-b, 13a-b.
Fabalicypris hungarica Kozur, 1985: 82, pl. 2, figs 2, 9, 10.

Bairdiacypris opulenta – Shi & Chen 1987: 51, pl. 13, fig. 10.

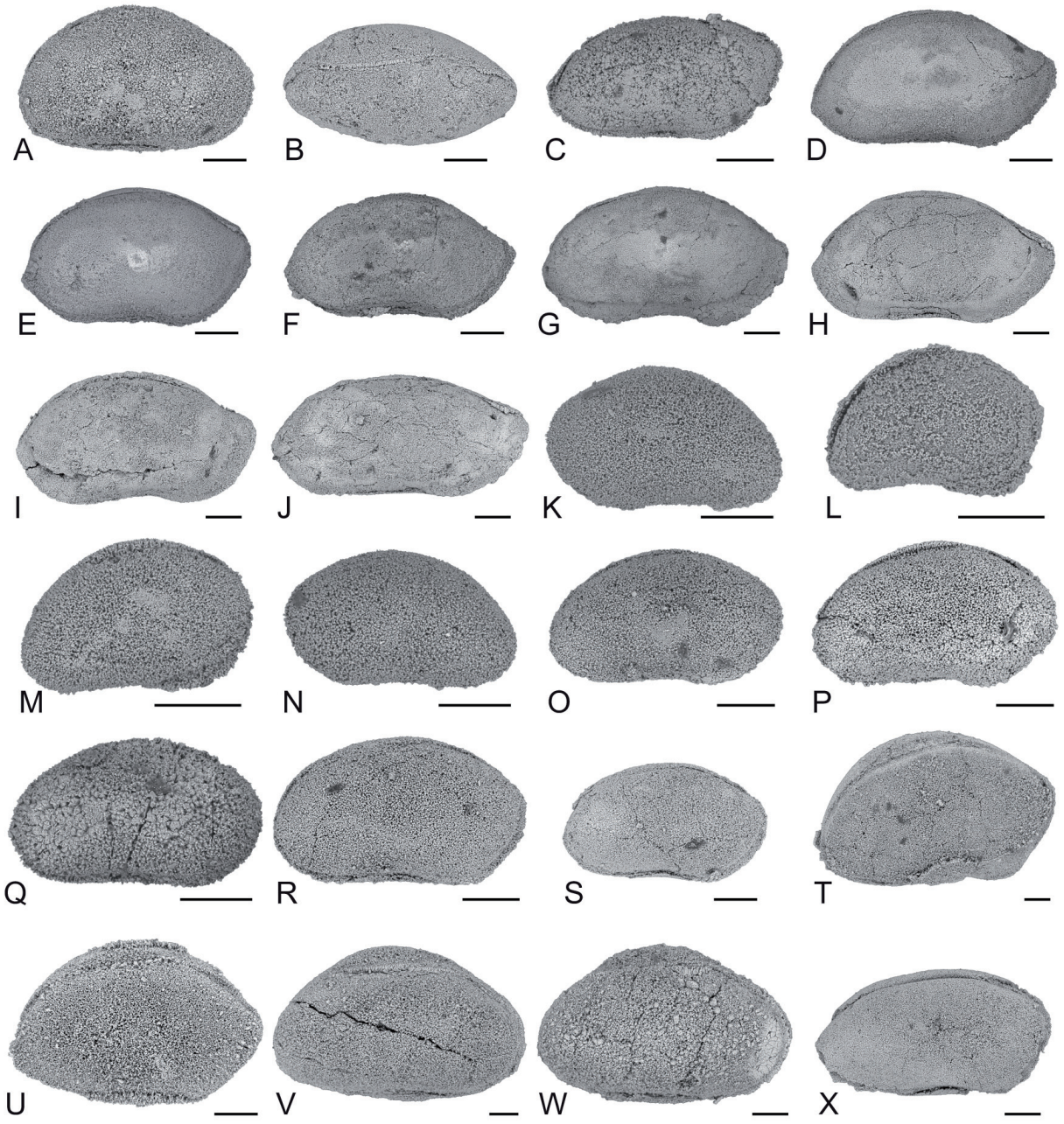

Fig. 7. Ostracods from the Dajiang section, South China. — **A–B**. *Bairdia* sp. 3. **A**. Carapace, right lateral view, P6M2963. **B**. Carapace, dorsal view, P6M2964. — **C**. *Bairdia* sp. 4, Carapace, right lateral view, P6M2965. — **D–J**. *Bairdia* sp. 5. **D**. Carapace, right lateral view, P6M2966. **E**. Carapace, right lateral view, P6M2967. **F**. Carapace, right lateral view, P6M2968. **G**. Carapace, right lateral view, P6M2969. **H**. Carapace, right lateral view, P6M2970. **I**. Carapace, right lateral view, P6M2971. **J**. Carapace, right lateral view, P6M2972. — **K–M**. *Bairdia*? sp. 6. **K**. Carapace, left lateral view, P6M2973. **L**. Carapace, right lateral view, P6M2974. **L**. Carapace, right lateral view, P6M2975. — **N–S**. *Bairdia* sp. 7. **N**. Carapace, left lateral view, P6M2976. **O**. Carapace, right lateral view, P6M2977. **P**. Carapace, right lateral view, P6M2978. **Q**. Carapace, right lateral view, P6M2979. **R**. Carapace, right lateral view, P6M2980. **S**. Carapace, right lateral view, P6M2981. — **T–U**. *Bairdia* sp. 8. **T**. Carapace, right lateral view, P6M2982. **U**. Carapace, right lateral view, P6M2983. — **V–W**. ?*Bairdia* sp. 8. **V**. Carapace, right lateral view, P6M2984. **W**. Carapace, right lateral view, P6M2985. — **X**. *Bairdia* sp. 9, carapace, right lateral view, P6M2986. – Scale = 100 µm.

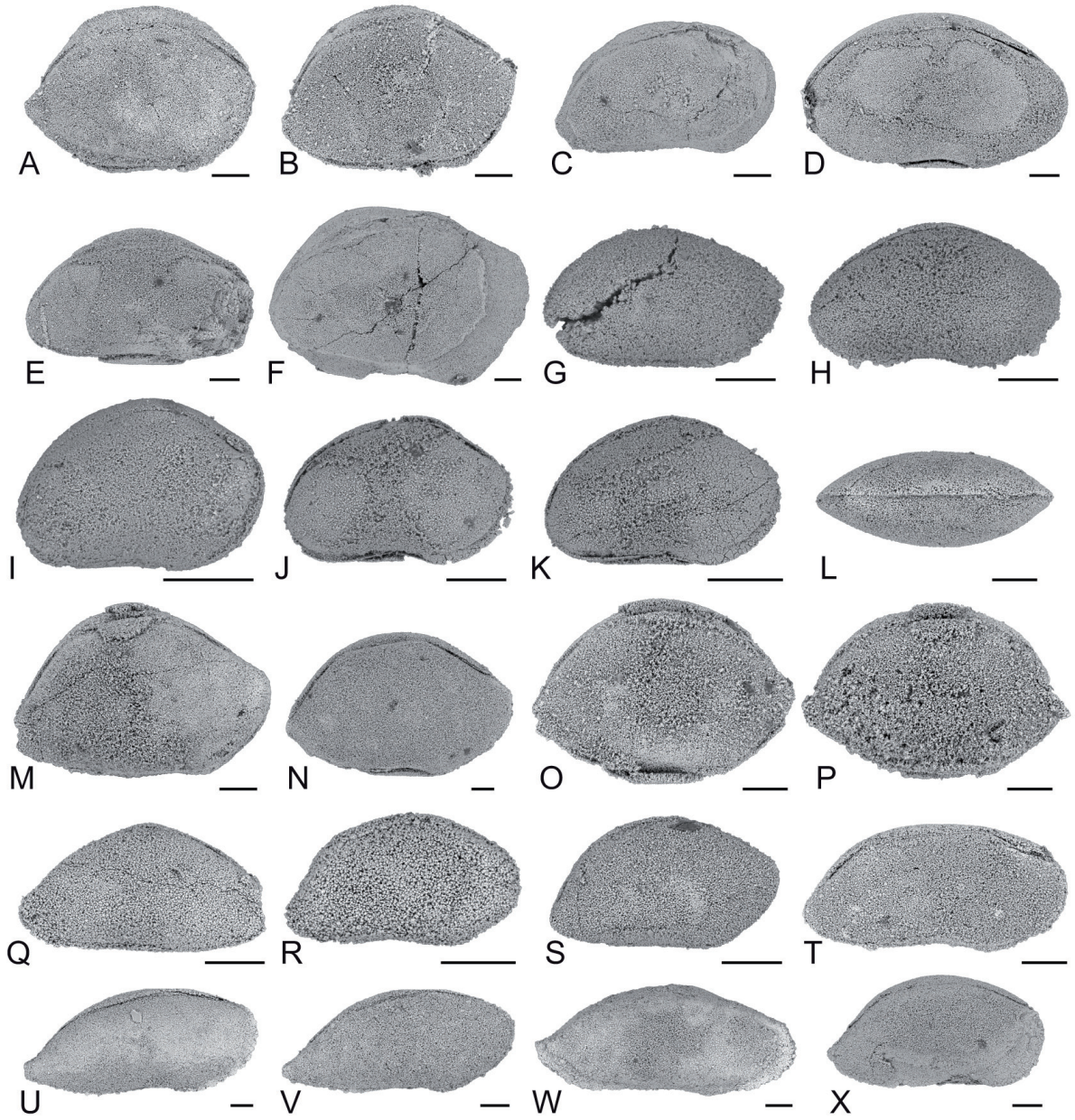

Fig. 8. Ostracods from the Dajiang section, South China. — **A**. *Bairdia* sp. 10, carapace, right lateral view, P6M2987. — **B**. *Bairdia* sp. 11, carapace, right lateral view, P6M2988. — **C**. *Bairdia* sp. 12, carapace, right lateral view, P6M2989. — **D**. *Bairdia* sp. 13, carapace, right lateral view, P6M2990. — **E**. *Bairdia* sp. 14, carapace, right lateral view, P6M2991. — **F**. *Bairdia* sp. 15, carapace, right lateral view, P6M2992. — **G**. *Bairdia* sp. 16, carapace, right lateral view, P6M2993. — **H**. *Bairdia* sp. 17, carapace, right lateral view, P6M2994. — **I–L**. *Bairdia* sp. 18. **I**. Carapace, right lateral view, P6M2995. **J**. Carapace, right lateral view, P6M2996. **K**. Carapace, right lateral view, P6M2997. **L**. Carapace, dorsal view, P6M2998. — **M–N**. *Bairdia* sp. 19. **M**. Carapace, right lateral view, P6M2999. **N**. Carapace, right lateral view, P6M3000. — **O–P**. *Bairdia* sp. 20. **O**. Carapace, right lateral view, P6M3001. **P**. Carapace, right lateral view, P6M3002. — **Q**. *Bairdia* sp. 21, carapace, right lateral view, P6M3003. — **R–S**. *Bairdia* sp. 22. **R**. Carapace, right lateral view, P6M3004. **S**. Carapace, right lateral view, P6M3005. — **T**. *Bairdia* sp. 23, carapace, right lateral view, P6M3006. — **U–W**. *Bairdia* sp. 24. **U**. Carapace, right lateral view, P6M3007. **V**. Carapace, right lateral view, P6M3008. **W**. Carapace, right lateral view, P6M3009. — **X**. *Bairdia* cf. sp. 24, carapace, right lateral view, P6M3010. – Scale = 100 μm.

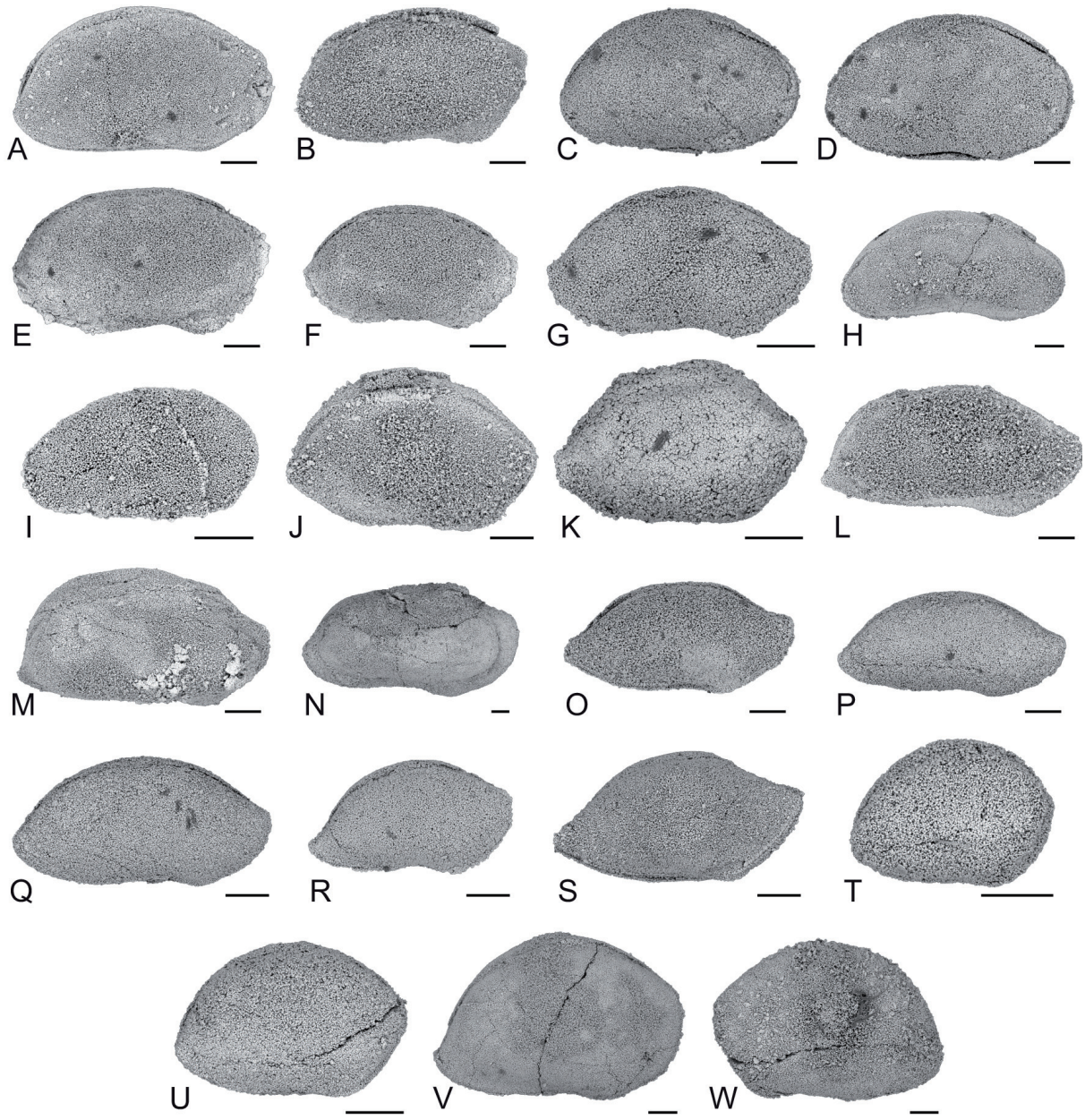

Fig. 9. Ostracods from the Dajiang section, South China. — **A–D**. *Bairdia* sp. 25. **A**. Carapace, right lateral view, P6M3011. **B**. Carapace, right lateral view, P6M3012. **C**. Carapace, right lateral view, P6M3013. **D**. Carapace, right lateral view, P6M3014. — **E–G**. *Bairdia* sp. 26. **E**. Carapace, right lateral view, P6M3015. **F**. Carapace, right lateral view, P6M3016. **G**. Carapace, right lateral view, P6M3017. — **H–I**. *Bairdia* sp. 27. **H**. Carapace, right lateral view, P6M3018. **I**. Carapace, right lateral view, P6M3019. — **J-K**. *Bairdia* sp. 28. **J**. Carapace, right lateral view, P6M3020. **K**. Carapace, right lateral view, P6M3021. — **L–N**. *Bairdia* sp. 29. **L**. Carapace, right lateral view, P6M3022. **M**. Carapace, right lateral view, P6M3023. **N**. Carapace, right lateral view, P6M3024. — **O–Q**. *Bairdia* sp. 30. **O**. Carapace, right lateral view, P6M3025. **P**. Carapace, right lateral view, P6M3026. **Q**. Carapace, right lateral view, P6M3027. — **R-S**. *Bairdia* sp. 31. **R**. Carapace, right lateral view, P6M3028. **S**. Carapace, right lateral view, P6M3029. — **T–W**. *Bairdia* sp. 32. **T**. Carapace, right lateral view, P6M3030. **U**. Carapace, right lateral view, P6M3031. **V**. Carapace, right lateral view, P6M3032. **W**. Carapace, left lateral view, P6M3033. – Scale = 100 µm.

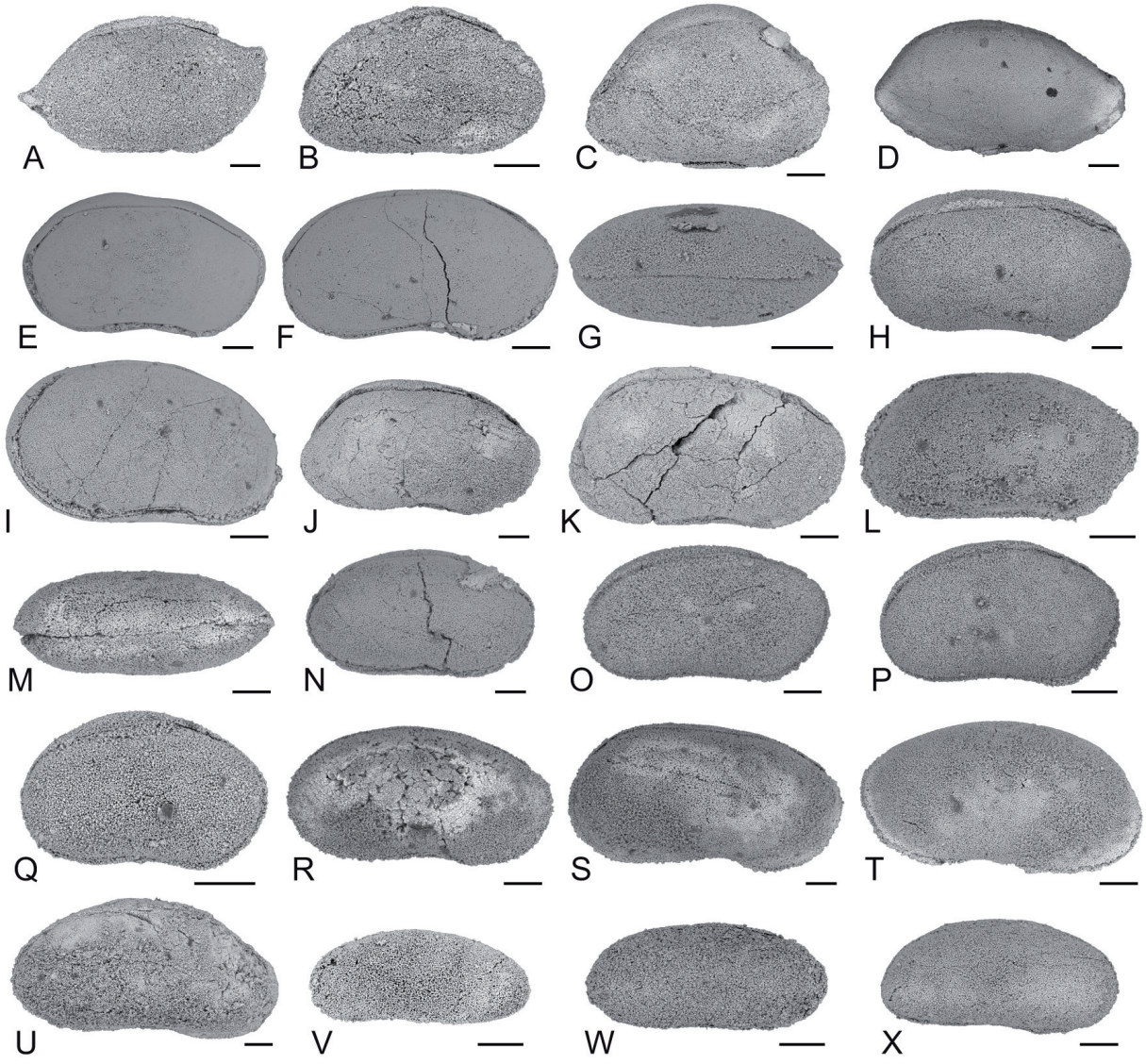

Fig. 10. Ostracods from the Dajiang section, South China. — **A**. *Bairdia* sp. 33, carapace, right lateral view, P6M3034. — **B**. *Bairdia* sp. 34, carapace, right lateral view, P6M3035. — **C**. *Bairdia* sp. 35, carapace, right lateral view, P6M3036. — **D**. *Bairdia*? sp. 36, carapace, right lateral view, P6M3037. — **E–H**. *Bairdiacypris ottomanensis* Crasquin–Soleau, 2004. **E**. Carapace, right lateral view, P6M3038. **F**. Carapace, right lateral view, P6M3039. **G**. Carapace, dorsal view, P6M3040. **H**. Carapace, right lateral view, P6M3041. — **I**. *Bairdiacypris* sp. 1, carapace, right lateral view, P6M3042. — **J–K**. *Bairdiacypris* sp. 2. **J**. Carapace, right lateral view, P6M3043. **K**. Carapace, right lateral view, P6M3044. — **L–M**. *Bairdiacypris* sp. 3. **L**. Carapace, right lateral view, P6M3045. **M**. Carapace, dorsal view, P6M3046. — **N–Q**. *Bairdiacypris* sp. 4. **N**. Carapace, right lateral view, P6M3047. **O**. Carapace, right lateral view, P6M3048. **P**. Carapace, right lateral view, P6M3049. **Q**. Carapace, right lateral view, P6M3050. — **R–T**. *Bairdiacypris* sp. 5. **R**. Carapace, right lateral view, P6M3051. **S**. Carapace, right lateral view, P6M3052. **T**. Carapace, left lateral view, P6M3053. — **U**. *Bairdiacypris*? sp. 6, carapace, right lateral view, P6M3054. — **V–X**. *Bairdiacypris* sp. 7. **V**. Carapace, right lateral view, P6M3055. **W**. Carapace, right lateral view, P6M3056. **X**. Carapace, right lateral view, P6M3057. – Scale = 100 μm.

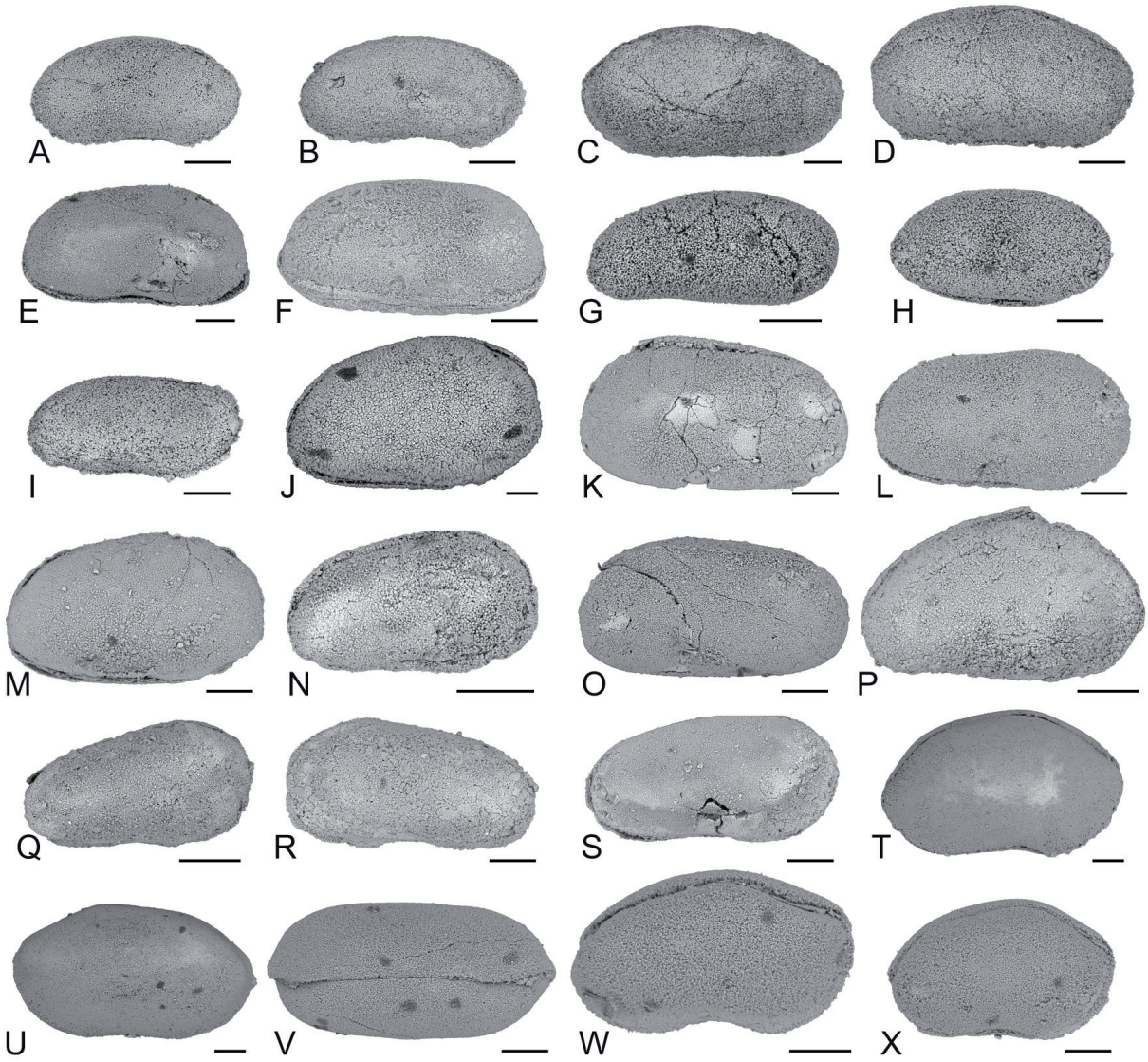

Fig. 11. Ostracods from the Dajiang section, South China. — **A–B**. *Bairdiacypris* sp. 8. **A**. Carapace, right lateral view, P6M3058. **B**. Carapace, right lateral view, P6M3059. — **C–D**. *Bairdiacypris* sp. 9. **C**. Carapace, right lateral view, P6M3060. **D**. Carapace, right lateral view, P6M3061. — **E–F**. *Bythocypris*? sp. 1. **E**. Carapace, right lateral view, P6M3062. **F**. Carapace, right lateral view, P6M3063. — **G**. *Bythocypris* sp. 2, carapace, right lateral view, P6M3064. — **H**. *Bythocypris*? sp. 3, carapace, right lateral view, P6M3065. — **I**. *Fabalicypris parva* Wang, 1978, carapace, right lateral view, P6M3066. — **J–N**. *Liuzhinia antalyaensis* Crasquin–Soleau, 2004. **J**. Carapace, right lateral view, P6M3067. **K**. Carapace, left lateral view, P6M3068. **L**. Carapace, left lateral view, P6M3069. **M**. Carapace, right lateral view, P6M3070. **N**. Carapace, right lateral view, P6M3071. — **O**. ?*Liuzhinia antalyaensis* Crasquin–Soleau, 2004, carapace, left lateral view, P6M3072. — **P**. *Liuzhinia* sp., carapace, right lateral view, P6M3073. — **Q–S**. *Liuzhinia* sp. 2. **Q**. Carapace, right lateral view, P6M3074. **R**. Carapace, left lateral view, P6M3075. **S**. Carapace, right lateral view, P6M3076. — **T–X**. *Orthobairdia jeanlouisi* sp. nov. **T**. Holotype, carapace, right lateral view, P6M3077. **U**. Carapace, left lateral view, P6M3078. **V**. Paratype, carapace, dorsal view, P6M3079. **W**. Carapace, right lateral view, P6M3080. **X**. Carapace, right lateral view, P6M3081. – Scale = 100 µm.

Fabalicypris parva – Crasquin-Soleau *et al.* 2004: 286, pl. 3, figs 4-5. — Mette 2008: pl. 2, fig. 8 - Crasquin *et al.* 2010: 353, fig. 9A'-B'.

Localities

- Wujiaping Formation (sample 05PAJ26), Dajiang section (25°33'56''N-106°39'41''E), Guizhou Province, South China, Changhsingian, Late Permian.
- Longtan and Changxing Formations, Guizhou and Yunnan Provinces, South China, Wuchiapingian and Changhsingian, Late Permian (Wang 1978).
- Bükk Mountains, Hungary, Late Moscovian, Carboniferous, Late Permian (Kozur 1985).
- Changxing formation, Meishan section, Zhejiang Province, South China, Changhsingian, Late Permian (Shi & Chen 1987; Crasquin *et al.* 2010).
- Çürük dağ section, Western Taurus, Turkey, Wuchiapingian and Changhsingian, Late Permian (Crasquin-Soleau *et al.* 2004).
- Zal section, Iran, Changhsingian, Late Permian (Mette 2008).

Remarks

According to previously published records of *Fabalicypris parva* Wang, 1978, this species is known from the Late Moscovian (Carboniferous; Kozur 1985) to the Changhsingian (Late Permian; Wang 1978; Shi & Chen 1987; Crasquin-Soleau *et al.* 2004; Mette 2008; Crasquin *et al.* 2010). This long stratigraphic range is suspicious: most of the occurrences being late Permian in age, the Carboniferous one seems questionable. When defining *F. hungarica* Kozur, 1985 as a synonym of *F. parva* Wang, 1978, Crasquin *et al.* (2010) stated that *F. hungarica* had a more rounded PB and a maximum of convexity located higher than *F. parva*. However, because all intermediate shapes between the 2 species were available, they considered all the specimens as belonging to the same species. This observation together with the long stratigraphic repartition of the species seems to indicate an evolutionary trend within one single species. More material is necessary to test this hypothesis.

Genus *Liuzhinia* Zheng, 1976

Liuzhinia antalyaensis Crasquin-Soleau, 2004
Fig. 11J-N

Liuzhinia antalyaensis Crasquin-Soleau, 2004: 286, pl. 3, figs 6-13.

Liuzhinia antalyaensis – Crasquin-Soleau *et al.* 2006: 62, pl. 3, figs 12-13. — Crasquin *et al.* 2008: 249, pl. 4, figs 9, 12.

Localities

- Samples 05PAJ30-33, 42, Daye Formation, Dajiang section (25°33'56''N-106°39'41''E), Guizhou Province, South China, Griesbachian, Early Triassic.
- Kokarkuyu Formation, Çürük dağ section, Western Taurus, Turkey, Early Triassic (Crasquin-Soleau *et al.* 2004).
- Jinya / Waili section, Fengshan area, Guangxi Province, South China, Griesbachian, Early Triassic (Crasquin-Soleau *et al.* 2006).
- Bulla section, Dolomites, Southern Alps, Northern Italy, Early Triassic (Crasquin *et al.* 2008).

Genus *Orthobairdia*, Sohn, 1960

Orthobairdia jeanlouisi sp. nov.
Fig. 11T-X

Diagnosis

Species of *Orthobairdia* with preplete carapace, sharp angles between PDB, DB and ADB (~150°) and large radius of curvature at AB and PB.

Etymology

Personal dedication to Jean-Louis Forel.

Material examined

Holotype

One carapace (Fig. 11T), sample 05PAJ43, collection number P6M3077.

Paratype

One carapace (Fig. 11V), sample 05PAJ43, collection number P6M3079.

Other material

13 carapaces, several fragments. The species is known from its type locality only.

Type locality

Daye Formation (samples 05PAJ43-45), Dajiang section (25°33’56”N-106°39’41”E), Guizhou Province, South China, Griesbachian, Early Triassic.

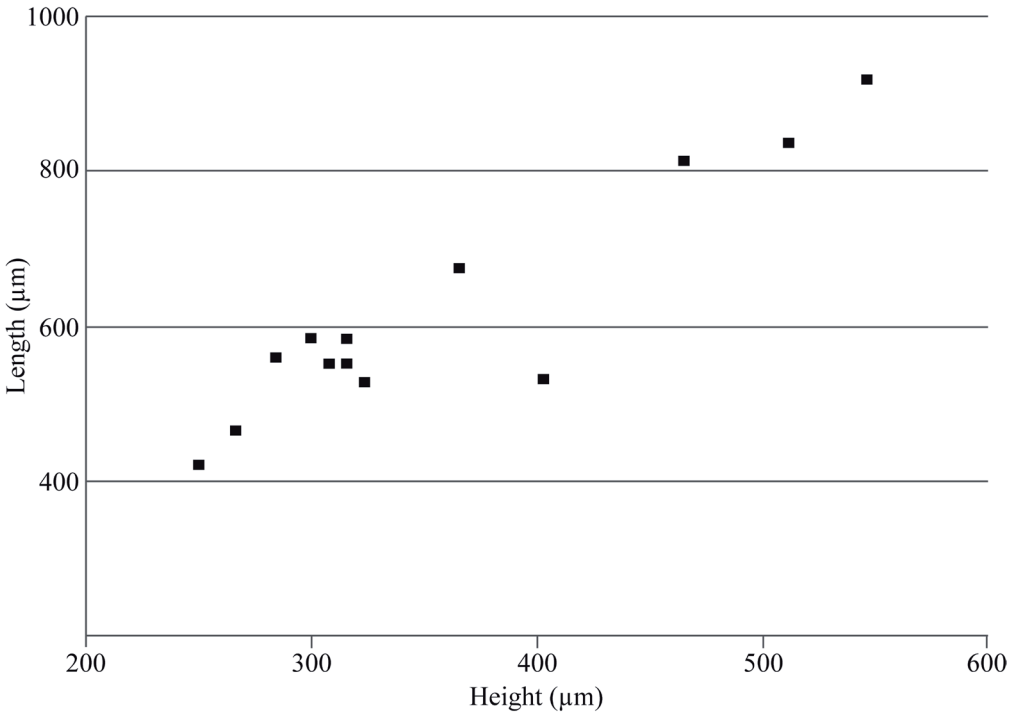

Fig. 12. Height/length diagram of *Orthobairdia jeanlouisi* sp. nov.

Measurements (Fig. 12)

L = 422 – 918 μm; H = 250 – 546 μm; H/L = 0.50 – 0.75.

Description

Carapace subtriangular in lateral view; surface smooth; LV overlapping RV all around the carapace, dorsal overlap thicker; angles between PDB, DB and ADB ~ 150° at both valves; PDB straight with steep backward slope; DB and ADB long, together ~ 60% of Lmax; DB straight at both valves, bent backward; ADB straight at LV, slightly convex at RV, less steep than PDB; VB concave; AVB long and gently rounded; PVB shorter, gently rounded; AB subtriangular, with large radius of convexity, maximum located above mid-H; PB subtriangular, sharply pointed, with narrower but still large radius of curvature, maximum located slightly below mid-H; carapace preplete; Lmax located at mid-H or slightly below.

Remarks

Orthobairdia jeanlouisi sp. nov. can be compared to *Orthobairdia texana* (Harlton, 1927) *sensu* Shi & Chen, 2002 from the Late Permian of Heshan and Yishen, Guangxi Province, South China (Shi & Chen 2002) but here the species is shorter, posterior maximum of convexity is clearly situated more dorsally, anterior part is more elongated, ADB steeper. *Orthobairdia jeanlouisi* sp. nov. is also close to *Orthobairdia exilimarginata* Chen, 1987 from the Changhsingian (Late Permian) of the Meishan section, Zhejiang Province, South China (Shi & Chen 1987), but the new species is less elongated and its DB is shorter and bent backward. This species can also be related to *Orthobairdia meishanensis* Chen, 1987 from the Permian of the Meishan section, Zhejiang Province, South China (Shi & Chen 1987), however, *Orthobairdia jeanlouisi* sp. nov. has the PB located higher, a shorter DB and a less steep PDB.

Family Pachydomellidae Berdan & Sohn, 1961
Genus *Microcheilinella* Geis, 1933

Microcheilinella cf. ***venusta*** Chen, 1958
Fig. 13Q

Locality

- Wujiaping Formation (samples 05PAJ22, 24, 25, 28, 29), Dajiang section (25°33’56’’N-106°39’41’’E), Guizhou Province, South China, Changhsingian, Late Permian.

Remarks

This species is closely related to *Microcheilinella venusta* Chen, 1958 from the Early Permian of Lungtan, Qixia Formation, Nankin (Chen 1958) but here the specimens are more elongated and thinner, with a more rounded PB. It can also be compared to *Microcheilinella* cf. *venusta* Chen, 1958 *sensu* Crasquin-Soleau, 2006 from the Early Triassic of the Jinya/Waili section, Guangxi Province, South China (Crasquin-Soleau *et al.* 2006). However here the species is more elongated, with longer DB and no lateral compression in the posterior part.

Superfamily Cypridacea Baird, 1845
Family Paracyprididae Sars, 1923
Genus *Paracypris* Sars, 1866

Paracypris gaetanii Crasquin-Soleau, 2006
Fig. 13T-X

Paracypris sp. Hao 1992: 42, pl. 1, fig. 24.
Paracypris gaetanii Crasquin-Soleau, 2006: 64, pl. 4, figs 1-4.

Paracypris sp. – Crasquin-Soleau & Kershaw 2005: pl. 1, figs 7-9.
Paracypris gaetanii – Crasquin *et al.* 2008: 249, pl. 4, fig. 12. — Forel *et al.* 2009: 819, fig. 4 (5). — Forel & Crasquin 2011: figs 3F', 4A.

Localities

- Wujiaping and Daye Formations (samples 05PAJ22, 31, 32, 35, 37-40), Dajiang section (25°33'56''N-106°39'41''E), Guizhou Province, South China, Changhsingian and Griesbachian, Late Permian and Early Triassic (Forel *et al.* 2009; this study).
- Feihsienkuan Formation, Zhenfeng, Guizhou Province, South China, Early Triassic (Hao 1992).
- Feixianguan Formation, Laolongdong section, Sichuan Province, South China, Induan, Early Triassic (Crasquin & Kershaw 2005).
- Jinya/Waili section, Fengshan area, Guangxi Province, South China, Griesbachian, Early Triassic (Crasquin-Soleau *et al.* 2006).
- Bulla section, Dolomites, Southern Alps, Northern Italy, Early Triassic (Crasquin *et al.* 2008).
- Yinkeng Formation, Meishan section, Zhejiang Province, South China, Griesbachian, Early Triassic (Forel & Crasquin 2011).
- Kokarkuyu Formation, Çürük dağ section, Western Taurus, Turkey, Induan, Early Triassic (Forel in progress).

Remarks

This taxon is one of the rare species which crosses the Permian – Triassic boundary.

Superfamily Cytheracea Baird, 1850
Family Cytherideidae Sars, 1925
Genus *Basslerella* Kellett, 1935

Basslerella tota Chen & Bao, 1986
Fig. 14O-Q

Basslerella tota Chen & Bao, 1986: 123, pl. 1, figs 31-32; pl. 4, figs 7-8.

Basslerella tota – Crasquin-Soleau *et al.* 2004: 288, pl. 4, figs 9-10 — Yi 2004: pl. 2, fig. 20.

Localities

- Wujiaping Formation (samples 05PAJ24, 26, 28), Dajiang section (25°33'56''N-106°39'41''E), Guizhou Province, South China, Changhsingian, Late Permian.
- Chisia formation, Jiangsu Province, South China, Early Permian (Chen & Bao 1986).
- Pamuçak Formation, Çürük dağ section, Western Taurus, Turkey, Late Permian (Crasquin-Soleau *et al.* 2004).
- Kongtonshan section, Fujian Province, South China, Late Permian (Yi 2004).

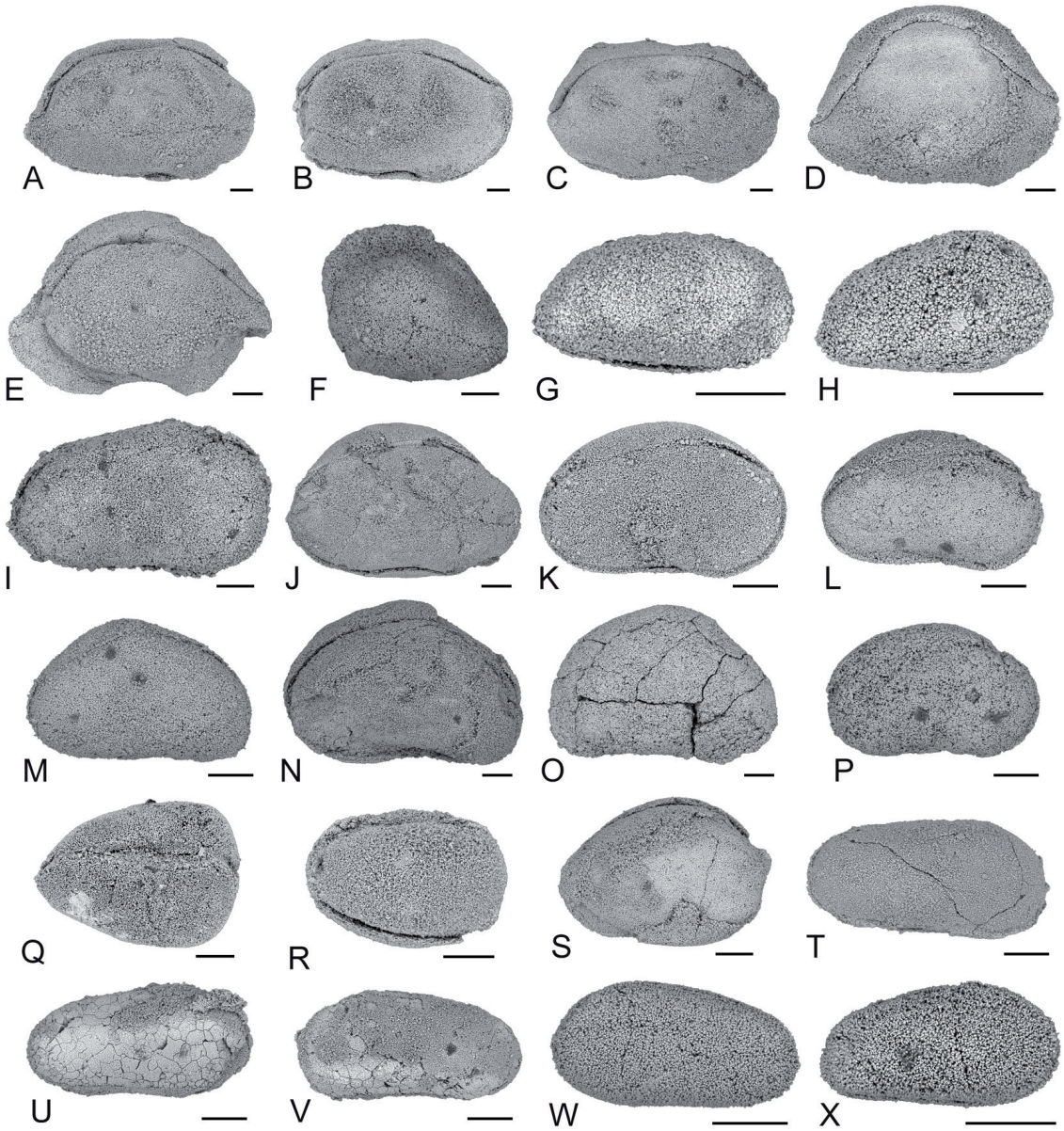

Fig. 13. Ostracods from the Dajiang section, South China. — **A–B**. *Petasobairdia* sp. 1. **A**. Carapace, right lateral view, P6M3082. **B**. Carapace, right lateral view, P6M3083. — **C**. *Petasobairdia* sp. 2, carapace, right lateral view, P6M3084. — **D–E**. *Petasobairdia* sp. 3. **D**. Carapace, right lateral view, P6M3085. **E**. Carapace, right lateral view, P6M3086. — **F**. *Petasobairdia*? sp. 4, carapace, right lateral view, P6M3087. — **G**. *Spinocypris* sp. 1, carapace, right lateral view, P6M3088. — **H–I**. *Spinocypris*? sp. 2. **H**. Carapace, right lateral view, P6M3089. **I**. Carapace, right lateral view, P6M3090. — **J**. *Kempfina* sp. 1, carapace, right lateral view, P6M3091. — **K–L**. *Silenites* sp. 1. **K**. Carapace, right lateral view, P6M3092. **L**. Carapace, right lateral view, P6M3093. — **M-N**. *Silenites* sp. 2. **M**. Carapace, right lateral view, P6M3094. **N**. carapace, right lateral view, P6M3095. — **O**. *Silenites* sp. 3, carapace, right lateral view, P6M3096. — **P**. *Silenites* sp. 4, carapace, right lateral view, P6M3097. — **Q**. *Microcheilinella* cf. *venusta* Chen, 1958, carapace, dorsal view, P6M3132. — **R**. *Microcheilinella* sp. 1, carapace, right lateral view, P6M3131. — **S**. *Cetollina*? sp. 1, carapace, right lateral view, P6M3098. — **T–X**. *Paracypris gaetanii* Crasquin–Soleau, 2006. **T**. Carapace, right lateral view, P6M3099. **U**. Carapace, right lateral view, P6M3100. **V**. Carapace, left lateral view, P6M3101. **W**. Carapace, left lateral view, P6M3102. **X**. Carapace, right lateral view, P6M3103. – Scale = 100 μm.

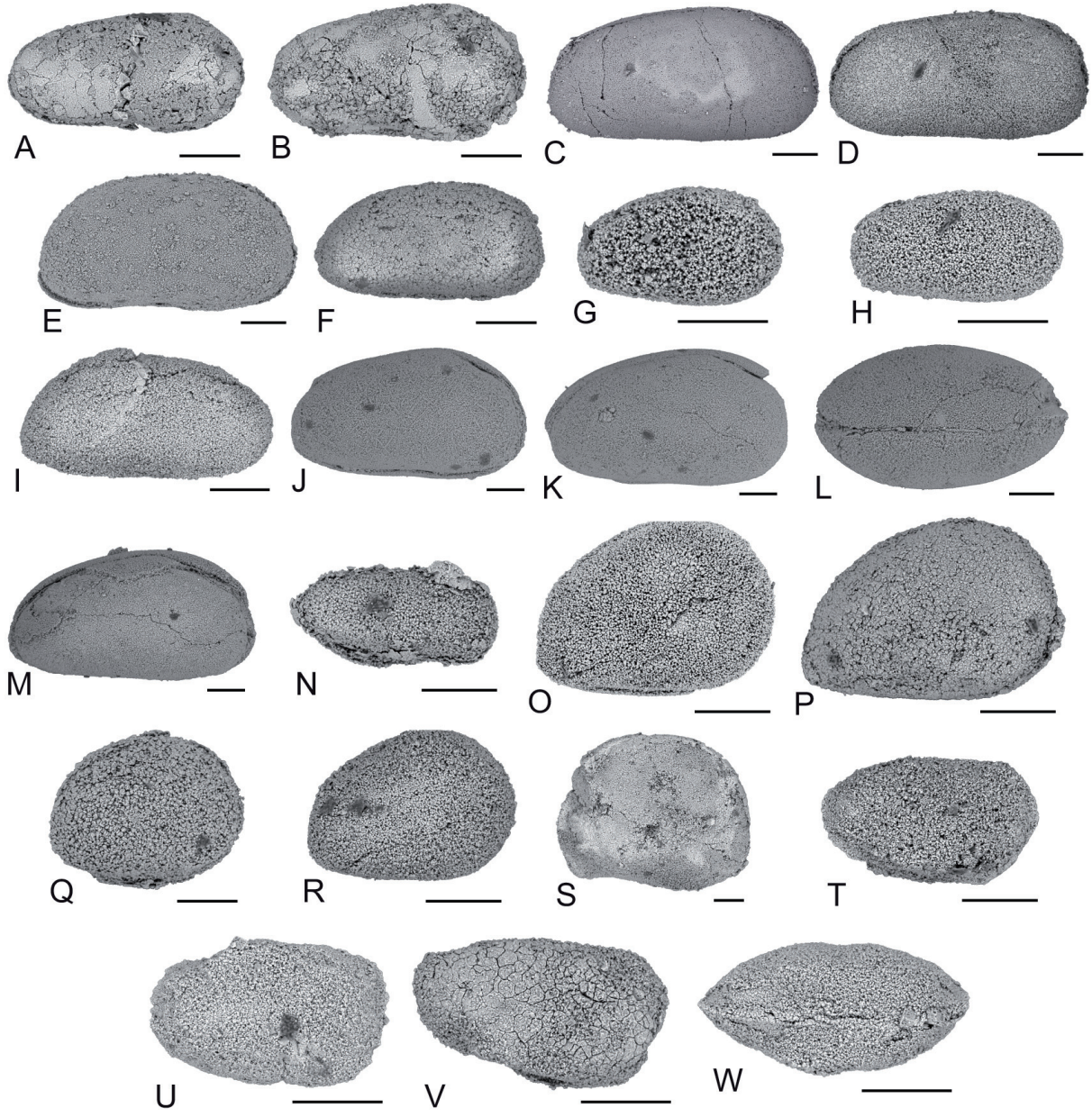

Fig. 14. Ostracods from the Dajiang section, South China. — **A–B**. *Paracypris* cf. *gaetanii* Crasquin–Soleau, 2006. **A**. Carapace, right lateral view, P6M3104. **B**. Carapace, right lateral view, P6M3105. — **C–E**. *Paracypris* sp. 6. **C**. Carapace, right lateral view, P6M3106. **D**. Carapace, right lateral view, P6M3107. **E**. Carapace, right lateral view, P6M3108. — **F**. *Paracypris* sp. 1, carapace, right lateral view, P6M3109. — **G**. *Paracypris*? sp. 2, carapace, right lateral view, P6M3110. — **H**. *Paracypris*? sp. 3, carapace, right lateral view, P6M3111. — **I**. *Paracypris*? sp. 4, carapace, right lateral view, P6M3112. — **J–M**. *Paracypris*? sp. 5. **J**. Carapace, right lateral view, P6M3113. **K**. Carapace, right lateral view, P6M3114. **L**. Carapace, dorsal view, P6M3151. **M**. Carapace, right lateral view, P6M3115. — **N**. *Monoceratina*? sp. 1, carapace, right lateral view, P6M3116. — **O–R**. *Basslerella tota* Chen & Bao, 1986. **O**. Carapace, right lateral view, P6M3117. **P**. Carapace, right lateral view, P6M3118. **Q**. Carapace, right lateral view, P6M3119. **R**. Carapace, right lateral view, P6M3120. — **S**. *Basslerella*? sp. 1, carapace, right lateral view, P6M3121. — **T–W**. *Callicythere postiangusta* Wei, 1981. **T**. Carapace, right lateral view, P6M3122. **U**. Carapace, right lateral view, P6M3123. **V**. Carapace, right lateral view, P6M3124. **W**. Carapace, dorsal view, P6M3125. – Scale = 100 µm.

Family Cytherissinellidae Kashevarova, 1958
Genus *Callicythere* Wei, 1981

Callicythere postiangusta Wei, 1981
Figs 14T-W, 15A-B

Callicythere postiangusta Wei, 1981: 504, pl. 1, figs 19-22.

Callicythere postiangusta – Crasquin-Soleau & Kershaw 2005: pl. 1, figs 1-6.

Localities

- Samples 05PAJ30, 31, 33, 35, 37, 38, 44, Daye Formation, Dajiang section (25°33'56''N-106°39'41''E), Guizhou Province, South China, Griesbachian, Early Triassic.
- Weiyuan, Leikoupo Formation, Sichuan Province, South China, Middle Triassic (Wei, 1981).
- Çürük dağ section, Western Taurus, Turkey, Early Triassic (Forel, in progress).
- Laolongdong section, Feixianguan Formation, Sichuan Province, South China, Early Triassic (Crasquin-Soleau & Kershaw, 2005).

Ostracod biodiversity variations

Ostracods are found from the top of the Wujiaping formation (05PAJ20) to the base of the Daye formation (05PAJ45). Of the 26 samples within this interval, 25 yielded ostracods. Species distribution is summarised in Fig. 2 and abundance and species richness variations are presented in Fig. 16A. In the productive samples, abundance varies from 1 (05PAJ36) to 2403 (05PAJ41) and species richness from 1 (05PAJ36) to 24 (05PAJ28). A taxa-specimen rarefaction analysis has been performed and suggests that communities have been well sampled and little sampling bias is expected. Several peaks (P) and drops (D) are distinguished on the biodiversity curves (Fig. 16A):

(1) Samples 05PAJ20 to 26 are relatively highly diversified, for both species richness and abundance (P1).
(2) This phase is followed by a sharp drop from 20 species in 05PAJ25 to 2 in 05PAJ27 (D1). 05PAJ27 records the minimum of Permian ostracod diversity in Dajiang.
(3) An important diversification is observed just before the Permian – Triassic boundary (PTB) (P2: 05PAJ28, 29). This peak is the maximum of species richness in Dajiang.
(4) Samples 05PAJ28 to 05PAJ30 (D2) bracket the PTB and show an important reduction of specific richness (from 24 to 3).
(5) Abundance and species richness then increase from 05PAJ31 to 05PAJ33 (P3). Species richness is however lower than in the Permian assemblages.
(6) Another reduction of diversity, both abundance and specific richness, is recorded in 05PAJ34-36 (D3).
(7) A slight rediversification is observed from 05PAJ37 to 05PAJ40 (P4).
(8) A reduction of species richness, together with a high abundance, is recorded in 05PAJ41 (D4).
(9) 05PAJ42 to 05PAJ45 (P5) show a slight rediversification of the assemblages. During this phase, species richness is relatively stable while abundance is low.

The biodiversity parameters in Dajiang show striking inversion through the PTB: high species richness/ low abundance for Permian assemblages, low species richness/ high to very high abundance in Triassic microbialites.

Composition of assemblages

Ostracods in Dajiang belong to 10 superfamilies/families, the distribution of which through the PTB is illustrated in Fig. 16B. The most abundant superfamily, both in the Permian and the Triassic, is Bairdioidea (encompassing the genera *Acratia*, *Bairdia*, *Bairdiacypris*, *Bythocypris*, *Fabalicypris*, *Kempfina*, *Liuzhinia*, *Microcheilinella*, *Orthobairdia*, *Petasobairdia*, *Silenites* and *Spinocypris*). It is absent from only 2 assemblages from D3 (05PAJ35, 36). Its proportions are between 20% (05PAJ37) and 100% of species (05PAJ27, 29, 45). The second most important superfamily is Cypridoidea (genus *Paracypris*). It is ubiquitous both in Permian and Triassic assemblages but shows higher proportions in Triassic assemblages. It is absent from 05PAJ20, 21, 26-29, 38, 44, 45. When it is present, it represents between

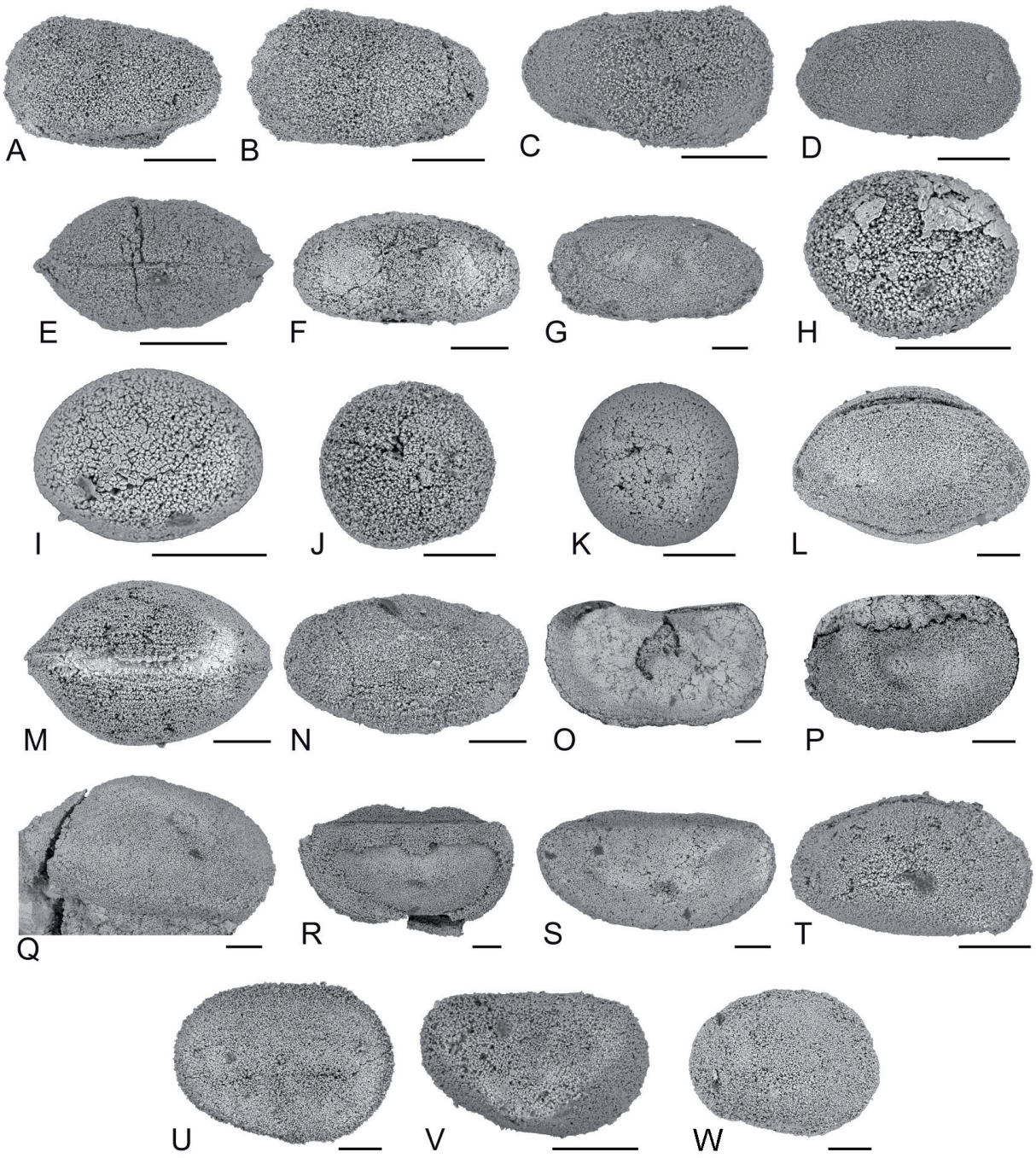

6% (05PAJ22) and 100% (05PAJ36) of the species. Cytheroidea (genera *Basslerella*, *Callicythere* and *Monoceratina*) are found both in Permian and Triassic assemblages. When it is present, it represents between 4% (05PAJ28) and 50% (05PAJ30, 35) of species. Paraparchitidae (genera *Paraparchites*, *Shemonaella*, Paraparchitiidae indet.) are present in 2 Permian assemblages and 1 Triassic: 05PAJ21 (11%), 05PAJ28 (4%), 05PAJ44 (9%). The following superfamilies/families only occur in the Permian: Cavellinidae (genera *Cavellina*, *Sulcella*) are found in only 3 assemblages of P1 (05PAJ21, 24, 25) where they represent between 5% (05PAJ25) and 11% of species (05PAJ21). Kirkbyoidea (genera *Amphissites*, *Kirkbya*, *Shleesha*) is part of 3 assemblages from P1 (05PAJ20, 22, 24) where it is respectively 14, 6 and 20% of the species. Polycopidae (genus *Polycope*) is present in 2 assemblages from P1: 05PAJ24 (7%) and 05PAJ25 (10%). Kloedenellidea (genus *Oliganisus*) is found in only one assemblage (05PAJ21) where it represents 11% of the species. Aparchitidae (genus *Cyathus*) is present in 2 assemblages: 05PAJ21 (11%) and 05PAJ28 (4%). Finally, only one species belongs to an undetermined superfamily/family (genus *Cetollina*). It is part of 05PAJ22 where it represents 6% of species.

In terms of species, the main extinction event occurs in the latest levels of the Wujiaping formation and the extinction rate is of 98%. Two species cross the PTB in Dajiang: *Bairdia jeromei* sp. nov. and *Paracypris gaetanii* Crasquin-Soleau, 2006 (Fig. 2). They are found in almost all microbialites, their last occurrences are high in the section (respectively 05PAJ41 and 05PAJ43). Two of the ten genera found in the microbialites have not been recorded in Permian strata before: *Callicythere* and *Orthobairdia*. Consequently, the faunal turnover is nearly complete at the specific level (94% of new species), partial at the generic level (20% of new genera) and no renewal is observed at the superfamily/family level. Importantly, most assemblages from the microbialites show high proportions of very small specimens (100 µm in length). These specimens belong to the same genera as the larger forms: hence the deviation of size is not due to the presence of intrinsically smaller genera. This aspect of the faunas will be addressed in future work.

Discussion

Palaeoenvironmental reconstruction

Most of the ostracods found in the Dajiang section are typical of intertropical warm settings (Crasquin-Soleau *et al.* 1999, 2004). The presence of *Polycope* could indicate the influence of cold waters (Kornicker 1959). The palaeoenvironmental preferences of Late Palaeozoic and Lower Triassic ostracods (Peterson

Fig. 15. (opposite page). Ostracods from the Dajiang section, South China. — **A–B**. *Callicythere postiangusta* Wei, 1981. **A**. Carapace, left lateral view, P6M3126. **B**. Carapace, left lateral view, P6M3127. — **C–E**. *Callicythere* sp. 1. **C**. Carapace, right lateral view, P6M3128. **D**. Carapace, right lateral view, P6M3129. **E**. Carapace, dorsal view, P6M3130. — **F**. *Sulcella* sp. 1, carapace, right lateral view, P6M3133. — **G**. *Sulcella*? sp. 2, carapace, right lateral view, P6M3134. — **H–I**. *Polycope* sp. 1. **I**. Carapace, right? lateral view, P6M3135. **J**. Carapace, right? lateral view, P6M3136. — **J**. *Polycope* sp. 2, carapace, right? lateral view, P6M3137. — **K**. *Polycope*? sp. 3, carapace, right? lateral view, P6M3138. — **L–M**. *Cyathus* sp. 1. **L**. Carapace, right lateral view, P6M3139. **M**. Carapace, dorsal view, P6M3140. — **N**. *Cyathus* sp. 2, carapace, right lateral view, P6M3141. — **O**. *Amphissites*? sp. 1, carapace, right lateral view, P6M3142. — **P**. *Amphissites*? sp. 2, broken carapace, right lateral view, P6M3143. — **Q**. *Shleesha*? sp. 1, broken carapace, right lateral view, P6M3144. — **R**. *Kirkbya*? sp. 1, carapace, right lateral view, P6M3145. — **S**. *Kirkbya*? sp. 2, carapace, right lateral view, P6M3146. — **T**. *Oliganisus*? sp. 1, carapace, left lateral view, P6M3147. — **U**. *Paraparchites* sp. 1, carapace, right lateral view, P6M3148. — **V**. Paraparchitidae indet., carapace, right lateral view, P6M3149. — **W**. *Shemonaella* sp. 1, carapace, left lateral view, P6M3150. – Scale = 100 µm.

& Kaesler 1980; Costanzo & Kaesler 1987; Melnyk & Maddocks 1988a, b; Crasquin-Soleau *et al.* 1999) found in Dajiang are summarized as follows (Fig. 16C):

(1) Euryhaline environments on the proximal platform (PP): Aparchitidae, Kloedenelloidea, Kirkbyoidea.
(2) Euryhaline environments, shallow to very shallow waters on the intermediate platform (IP): Cavellinidae, Cytherideidae, Paracyprididae, Paraparchitidae.
(3) Open carbonate environments with normal salinity and oygenation on the distal platform (DP): Acratiidae, Bairdiidae, Pachydomellidae.
(4) External zone of the distal platform (EDP): Bythocytheridae, Cytherissinellidae.
(5) Any platform environment, in normal salinity: *Polycope*.

The palaeobathymetric setting is estimated by the composition of assemblages regarding the five palaeoenvironmental groupings. Each bathymetrical zone is marked by the relative dominance of the corresponding group, while relative abundances of the other groups give information about the positioning within the zone determined by the dominant group.

DP forms are found all along the section and are always more than 50% of the assemblages (Fig. 16C). They indicate an open marine environment both in Late Permian and Early Triassic microbialites in Dajiang. PP forms only occur in Permian assemblages (05PAJ20-22, 24, 28). IP forms show the same pattern (05PAJ21, 24-26, 28) with one Triassic occurrence (05PAJ44). This documents proximal and variable conditions in the Permian of Dajiang, in the internal part of the circalittoral stage. EDP forms appear significantly in the first Triassic assemblage and are found throughout the microbialites. This suggests that the environmental stabilisation through the PTB can be related to a transgressive trend. *Polycope* are found only in Permian assemblages together with the unique Permian occurrence of EDP forms. This co-existence records a marked deepening of the area, associated with the possible influence of cold waters. The quasi-absence of PP and IP forms in the microbialites indicates a relative environmental stability in the deep external circalittoral zone, as revealed by the overwhelming dominance of DP forms and with significant components of EDP forms.

Worthy to note is the co-occurrence in assemblages 05PAJ25 and 44 of IP and EDP forms, indicating very different environmental settings. This record is best explained by considering that ecological classes used in this study not only reflect bathymetry but more generally the stability of the environmental parameters, here salinity, oxygenation and water depth. The punctual co-occurrence of these IP and EDP therefore seems to be related to the decoupling of environmental factors.

In summary, ostracod data provide additional evidence for the open-marine context through the entire PTB interval in Dajiang (Lehrmann *et al.* 2005). The shallow-subtidal, open-marine platform environment with relatively low to moderately high current energy of the Wujiaping formation is documented by ostracod faunas. However, the transgressive trend described here is discordant compared to the sedimentological proxy that indicates environments similar to the underlying Permian skeletal packstone. This discrepancy can be related to the fact that wave action has been reconstructed based on interbedded molluscan grainstone, which may only be episodic phenomenon (Lehrmann *et al.* 2005).

Contribution to the debate on oxygenation

As stated above, oxygenation of marine waters surrounding microbialites is an important challenge to understand their build-up mechanisms and the survival/recovery phenomenon following the extinction. In our former work addressing ostracod faunas of the PTB transition in Dajiang, we used the traditional Lethiers & Whatley model (Lethiers & Whatley 1994) to estimate the oxygen concentration at the base of the water column (Forel *et al.* 2009). This tool is now highly questioned and it is no longer possible to use it (e.g. Brandão & Horne 2009), but we can get a qualitative idea of the water oxygenation

independently. Most Permian and Triassic assemblages from Dajiang are dominated by Bairdioidea (being more than 50% of species, except in 05PAJ30, 35-37, 40, 41; Forel in press). This superfamily has been associated throughout its history with normal oxygenation settings (Pr R. Maddocks, Univ. of Houston, pers. comm.), so its dominance is a witness of good oxygenation at the base of the water

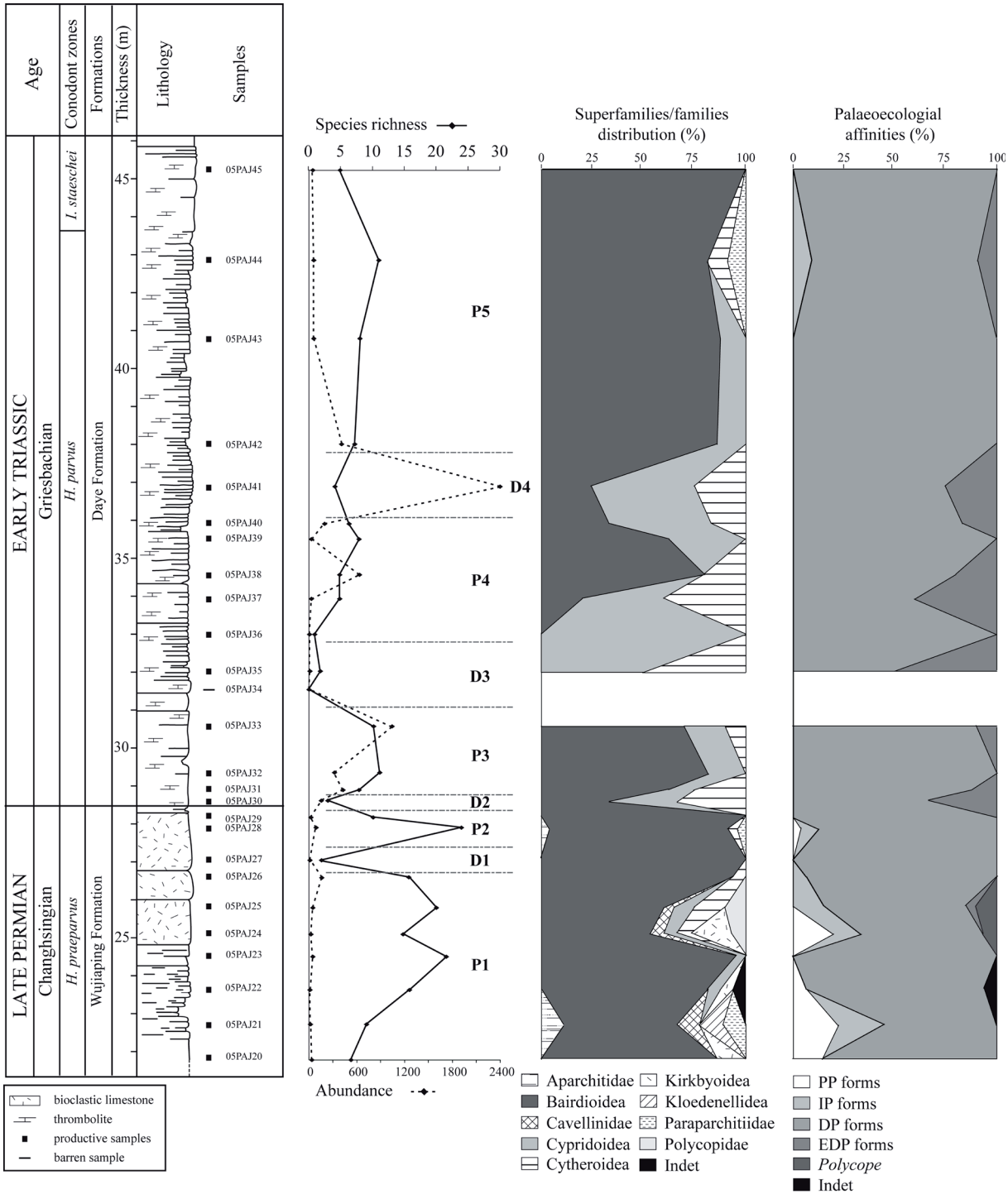

Fig. 16. Evolution of the ostracod faunas through the PTB in Dajiang. **A**. Evolution of the number of species (species richness) and number of specimens (abundance). **B**. Evolution of the relative proportions of each superfamily/family. **C**. Evolution of the relative proportions of each palaeoecological group.

column. The assemblages where Bairdioidea no longer represent the majority yielded high proportions of Cypridoidea that have similar requirements regarding oxygen levels (Pr R. Maddocks, Univ. of Houston pers. comm.). Although the setting through the PTB in Dajiang appears as normoxic, the biodiversity changes described above undeniably indicate deep ecological modifications. They should be linked to the relative degradation of the environment, buffered by the refuge created by the microbial ecosystem (Forel in press). These peculiar assemblages are recognised in all microbialites bearing sections analysed until now while they are absent from synchronous non-microbial deposits from deeper settings such as at the Meishan section, Global Stratotype Section and Point of the PTB (Crasquin *et al.* 2010; Forel & Crasquin 2011). They are intimately linked to the presence of microbialites (*i*) in space, areas lacking microbial mats are devoid of ostracods, (*ii*) in time, faunas disappearing with microbialites (e.g. Forel *et al.* in press; Forel in press).

Note on palaeo-geographical distributions and marine ostracods dispersal ways

Several species of this study display a wide distribution around both the Palaeo-Tethys and Neo-Tethys Oceans: *Bairdiacypris* Crasquin-Soleau, 2004, *Liuzhinia antalyaensis* Crasquin-Soleau, 2004, *Paracypris gaetanii* Crasquin-Soleau, 2006, *Basslerella tota* Chen & Bao, 1986, *Callicythere postiangusta* Wei, 1981. Because benthic ostracods have no pelagic stage, their migration is performed actively through locomotion and/or passively by the bottom currents. Their carbonate carapaces exclude them from depths below the lysocline, their migration is achieved on routes above this level. Their dispersal relies on the constancy of favourable environmental parameters of water-masses on their route, e.g. oxygen content, salinity, temperature.

However, active transoceanic dispersal potential of recent forms is relatively limited. Eggs, juveniles and adults would therefore be passively carried by wind, birds, fish, drifting algae or oceanic currents (Van Morkhoven 1962; Sandberg 1964; Teeter 1973; Whatley 1988; Babinot & Colin 1992; Lethiers & Crasquin-Soleau 1995). The characteristics of eggs of marine ostracods set some limits to this dissemination mode. Whereas eggs of freshwater ostracods are double-walled, those of marine ostracods are single-walled and do not stand desiccation (Kesling 1961), excluding dispersal by birds and winds (Teeter 1973). Larvae and adults are less sensitive to wind transportation because of their bigger size but would probably not withstand it (Teeter 1973). Although Kornicker & Sohn (1971) showed the possibility for adult freshwater ostracods ingested by fish to survive, it is unlikely that marine forms would have the same resistance. Aquatic plants could also be an important transportation vector for ostracods. Teeter (1973) found living specimens of *Hemicytherura cranekeyensis* Puri, 1960 on the marine algae *Turbinaria* Lamouroux, 1825 from Honduras. These algae often break into pieces that can float very far from the coast. Living ostracods have also been observed on the algae *Sargassum* Agardh, 1820. *Turbinaria* and *Sargassum* are found in the tropical area of Atlantic and Pacific Oceans. Once floating they could drift under the influence of surface currents to climatic zones favorable or not to the survival of the commensal ostracods. Most of the living ostracods have a high degree of flexibility and ecological tolerance so they should have a high capacity to successfully invade new environments.

Acknowledgements

This study is part of IGCP 572 'Restoration of Marine Ecosystems following the Permian–Triassic Mass Extinction: lessons for the present' and was undertaken with the support of the French CNRS Research Team UMR 7207 CR2P and the Chinese programs NSFC (40839903 and 40921062) and 111 (B08030). I am deeply indebted to my PhD supervisor Dr. Sylvie Crasquin (CNRS – CR2P) for her availability and great help in this study. I thank Prof. Feng Qinglai (China University of Geosciences, Wuhan) for his help during fieldwork on the Dajiang section. I also thank Martine Fordant (UPMC, Paris) for the processing of material and Alexandre Lethiers (UPMC, Paris) for his help with the illustrations. I am also grateful to Dr. Carys Bennett (Universite de Lille, France) and Dr. Vincent Perrier (University of

Tartu, Estonia) for their critical reviews and constructive suggestions, which have greatly improved the quality of this analysis.

References

Babinot J.F. & Colin J.P. 1992. Marine ostracode provincialism in the Late Cretaceous of the Tethyan realm and the Austral Province. *In*: Malmgren B.A. & Bengtson P. (eds) *Biogeographic patterns in the Cretaceous ocean. 5th biannual meeting of the European Union of Geosciences Symposium on Biogeographic patterns in the Cretaceous ocean*: 283-293. Strasbourg, France.

Benton M.J. & Twitchett R.J. 2003. How to kill (almost) all life: the end-Permian extinction event. *Trends in Ecology & Evolution* 18: 358-365.

Bond D.P.G., Wignall P.B., 2010. Pyrite framboid study of marine Permo-Triassic boundary sections: a complex anoxic event and its relationship to contemporaneous mass extinction. *Geological Society of America Bulletin* 122: 1265-1279. http://dx.doi.org/ 10.1130/B30042.1

Brandão S.N. & Horne D.J. 2009. The Platycopid Signal of oxygen depletion in the ocean: a critical evaluation of the evidence from modern ostracod biology, ecology and depth distribution. *Palaeogeography, Palaeoclimatology, Palaeoecology* 283: 126-133. http://dx.doi.org/10.1016/j.palaeo.2009.09.007

Chen D.Q. & Bao H. 1986. Lower Permian Ostracodes from the Chihsia Formation of Jurongan Longtar, Jiangsu Province. *Acta Micropalaeontologica Sinica* 3: 107-132.

Chen L., Wang Y., Xie S., Kershaw S., Dong M., Yang H., Liu H., Algeo T.J. 2011. Molecular records of microbialites following the end-Permian mass extinction in Chongyang, Hubei Province, South China. *Palaeogeography, Palaeoclimatology, Palaeoecology* 308: 151-159. http://dx.doi.org/10.1016/j.palaeo.2010.09.010

Chen T.C. 1958. Permian ostracods from the Chihsia limestone of Lungtan, Nanking. *Acta Palaeontologica Sinica* 6: 215-257.

Costanzo G.V. & Kaesler R.L. 1987. Changes in Permian marine Ostracode faunas during regression, Florena Shale, Northeastern Kansas. *Journal of Paleontology* 61: 1204-1215.

Crasquin S., Forel M.B., Feng Q., Yuan A., Baudin F. & Collin P.Y. 2010. Ostracods (Crustacea) through the Permian-Triassic boundary in South China: the Meishan stratotype (Zhejiang Province). *Journal of Systematic Palaeontology* 8: 331-370. http://dx.doi.org/10.1080/14772011003784992

Crasquin S., Perri M.C., Nicora A. & De Wever P. 2008. Ostracods across the Permian – Triassic boundary in Western Tethys: the Bulla parastratotype (Southern Alps). *Rivista Italiana di paleontologia e Stratigrafia* 114: 235-264.

Crasquin-Soleau S., Broutin J., Roger J., Platel J.-P., Al Hashmi A., Angiolini L., Baud A., Bucher H. & Marcoux J. 1999. First Permian ostracode fauna from the Arabian Plate (Khuff Formation, Sultanate of Oman). *Micropaleontology* 45: 163-182.

Crasquin-Soleau S., Galfetti T. & Bucher H. 2006. Early Triassic ostracods from South China. *Rivista Italiana di Paleontologia e Stratigrafia* 112: 55-75.

Crasquin-Soleau S. & Kershaw S. 2005. Ostracod fauna from the Permian-Triassic boundary interval of South China (Huaying Mountains, eastern Sichuan Province): palaeoenvironmental significance. *Palaeogeography, Palaeoclimatology, Palaeoecology* 217: 131-141. http://dx.doi.org/10.1016/j.palaeo.2004.11.027

Crasquin-Soleau S., Marcoux J., Angiolini L., Richoz S., Nicora A., Baud A. & Bertho Y. 2004. A new ostracode fauna from the Permian-Triassic boundary in Turkey (Taurus, Antalya Nappes). *Micropaleontology* 50: 281-296.

Crasquin-Soleau S., Vaslet D. & Le Nindre Y.M. 2005. Ostracods as markers of the Permian/Triassic boundary in Khuff Formation of Saudi Arabia. *Palaeontology* 48: 853-868. http://dx.doi.org/10.1111/j.1475-4983.2005.00476.x

Erwin D.H. 1993. *The Great Paleozoic Crisis: Life and Death in the Permian*. Columbia University Press, New York.

Forel M.B. in press. The Permian-Triassic mass extinction: ostracods (Crustacea) and microbialites. *Comptes Rendus Geoscience*.

Forel M.B. & Crasquin S. 2011. Lower Triassic ostracods (Crustacea) from Meishan section, Permian – Triassic GSSP (Zhejiang Province, South China). *Journal of Systematic Palaeontology* 9: 455-466. http://dx.doi.org/10.1080/14772019.2010.526638

Forel M.B., Crasquin S., Hips K., Kershaw S., Collin P.Y., Haas J. in press. Ostracods (Crustacea) from the Permian-Triassic Boundary of Bükk Mountains (Hungary). *Acta Paleontologica Polonica.*

Forel M.B., Crasquin S., Kershaw S., Feng Q.L. & Collin P.Y. 2009. Ostracods (Crustacea) and water oxygenation in earliest Triassic of South China: implications for oceanic events of the end-Permian mass extinction. *Australian Journal of Earth Sciences* 56: 815-823. http://dx.doi.org/10.1080/08120090903002631

Hao W.C. 1992. Lower Triassic marine ostracods from Guizhou. *Acta Micropaleontologica Sinica* 9: 37-44.

Kershaw S., Crasquin S., Li Y., Collin P.Y., Forel M.B., Mu X., Baud A., Wang Y., Xie S., Guo L., Maurer F. 2012. Microbialites and global environmental change across Permian – Triassic boundary: a synthesis. *Geobiology* 10 (1): 25-47. http://dx.doi.org/10.1111/j.1472-4669.2011.00302.x

Kershaw S., Li, Y., Crasquin-Soleau S., Feng Q., Mu X., Collin P.Y., Reynolds A., Guo L., 2007. Earliest Triassic microbialites in the South China block and other areas: control on their growth and distribution. *Facies* 53: 409-425. http://dx.doi.org/10.1007/s10347-007-0105-5

Kesling R.V. 1961. Morphology of living Ostracodes. *In*: Moore R.C. (ed.) *Arthropoda 3. Crustacea, Ostracoda: Q3–Q17*. Geological Society of America and University of Kansas Press; Boulder, Lawrence.

Kornicker L.S. 1959. Distribution of the ostracode suborder Cladocopa and a new species from the Bahamas. *Micropaleontology* 5: 69-75.

Kornicker L.S. & Sohn I.G. 1971. Viability of Ostracode Eggs Egested by Fish and Effect of Digestive Fluids on Ostracode Shells - Ecologic and Paleoecologic Implications. *Bulletin Centre Recherche Pau - SNPA* 5: 125-135.

Kozur H. 1985. Neue ostracoden-Arten aus dem oberen Mittelkarbon (Höheres Moskovian) Mittel- und Oberperm des Bükk-Gebirges (N-Ungarn*). Geologisch-Paläontologische Mitteilungen* 2: 1-145.

Lehrmann D.J. 1999. Early Triassic calcimicrobial mounds and biostromes of the Nanpanjiang basin, South China. *Geology* 27 (4): 359-362. http://dx.doi.org/10.1130%2F0091-7613%281999%29027%3C0359%3AETCMAB%3E2.3.CO%3B2

Lehrmann D.J., Payne J.L., Enos P., Montgomery P., Wei J., Yu Y., Xiao J. & Orchard M.J. 2005. Field excursion 2: Permian-Triassic boundary and a Lower-Middle Triassic boundary sequence on the Great Bank of Guizhou, Nanpanjiang basin, southern Guizhou Province. *Albertiana* 33: 169-186.

Lehrmann D.J., Payne J.L., Felix S.V., Dillett P.M., Wang H., Yu Y. & Wei J. 2003. Permian-Triassic boundary sections from shallow-marine carbonate platforms of the Nanpanjiang basin, south China: implications for oceanic conditions associated with the end-Permian extinction and its aftermath. *Palaios* 18: 138-152. http://dx.doi.org/10.1669%2F0883-1351%282003%2918%3C138%3APBSFSC%3E2.0.CO%3B2

Lethiers F. & Crasquin-Soleau S. 1988. Comment extraire des microfossiles à tests calcitiques de roches calcaires dures. *Revue de Micropaléontologie* 31: 56-61.

Lethiers F. & Crasquin-Soleau S. 1995. Distribution des ostracodes et paléocourantologie au Carbonifère terminal-Permien. *Geobios* 17: 257-272.

Lethiers F. & Whatley R. 1994. The use of Ostracoda to reconstruct the oxygen levels of the Late Paleozoic oceans. *Marine Micropaleontology* 24: 57-69.

Liao W., Wang Y., Kershaw S., Weng Z., Yang H. 2010. Shallow-marine dysoxia across the Permian-Triassic boundary: evidence from pyrite framboids in the microbialite in South China. *Sedimentary Geology* 232: 77-83.

Melnyk D.H. & Maddocks R.F. 1988a. Ostracode biostratigraphy of the Permo-Carboniferous of central and north-central Texas, Part I: paleoenvironmental framework. *Micropaleontology* 34: 1-20.

Melnyk D.H. & Maddocks R.F. 1988b. Ostracode biostratigraphy of the Permo-Carboniferous of central and north-central Texas, Part II: ostracode zonation. *Micropaleontology* 34: 21-40.

Mette W. 2008. Upper Permian and lowermost Triassic stratigraphy, facies and ostracods in NW Iran - implications for the P/T extinction event. *Stratigraphy* 5: 205-219.

Payne J.L. & Clapham M.E. 2012. End-Permian Mass Extinction in the Oceans: An Ancient Analog for the Twenty-First Century? *Annual Review of Earth and Planetary Sciences* 40: 89-111.

Peterson R.M. & Kaesler R.L. 1980. Distribution and diversity of ostracodes assemblages from the Hamlin Shale and the Americus limestones (Permian, Wolfcampian) in northern Kansas. *University of Kansas Paleontological Contributions* 100: 1-26.

Sandberg P.A. 1964. The Ostracod genus *Cyprideis* in the Americas. *Stockholm Contributions in Geology* 7.

Sepkoski J.J.J. 1984. A kinetic model of Phanerozoic taxonomic diversity; III, Post Paleozoic families and mass extinctions. *Paleobiology* 10 (2): 246-267.

Shi C.G. & Chen D.Q. 1987. The Changhsingian ostracodes from Meishan, Changxing, Zhejiang. *Stratigraphy and Palaeontology of Systemic Boundaries in China; Permian and Triassic Boundary* 5: 23-80 [in Chinese with English abstract].

Shi C.G. & Chen D.Q. 2002. Late Permian ostracodes from Heshan and Yishan of Guangxi. *Bulletin of the Nanjing Institute of Geology and Paleontology* 15: 47-129 [in Chinese with English abstract].

Song H.J., Tong J., Chen Z.Q., Yang H. & Wang Y.B. 2009. End-Permian mass extinction of foraminifers in the Nanpanjiang Basin, South China. *Journal of Paleontology* 83: 718-738.

Teeter J.W. 1973. Geographic distribution and dispersal of some recent shallow water marine Ostracoda. *Ohio Journal of Science* 73 (1): 46-54.

Van Morkhoven F.P. 1962. *Post Paleozoic Ostracoda. Their morphology, taxonomy and economic use. 1- General*. Elsevier, Amsterdam.

Wang S. 1978. Late Permian and Early Triassic ostracods of Western Guizhou and Northeastern Yunnan. *Acta Palaeontologica Sinica* 17: 277-308.

Wei M. 1981. Early and Middle Triassic Ostracods from Sichuan. *Acta Palaeontologica sinica*, 20 (6): 501-510 [in Chinese with English abstract].

Whatley R.C. 1988. Ostracoda and paleogeography. *In*: De Deckker P., Colin J.P. & Peypouquet J.P. (eds) *Ostracoda in Earth Sciences*: 103-123. Elsevier, Amsterdam.

Yang H., Chen Z.Q., Wang Y., Tong J., Song H., Chen J. 2011. Composition and structure of microbialite ecosystems following the end-Permian mass extinction in South China. *Palaeogeography, Palaeoclimatology, Palaeoecology* 308: 111-128. http://dx.doi.org/10.1016/j.palaeo.2010.05.029

Yi W. 2004. Ostracodes from the Upper Permian and Lower Triassic at the Kongtongshan scetion of Datian, Fujian. *Acta Palaeontologica Sinica* 43: 556-570.

Yin H., Wu S., Ding M., Zhang K., Tong J., Yang F. & Lai X. 1996. The Meishan section, candidate of the Global Stratotype Section and Point of Permian-Triassic boundary. *In*: Yin H.F (ed.) *The Paleozoic-Mesozoic Boundary Candidates of the Global Stratotype Section and Point of the Permian-Triassic Boundary*: 31-48. China University of Geosciences Press, Wuhan.

Manuscript received: 3 April 2012
Manuscript accepted: 26 June 2012
Published on: 1 August 2012
Topic editor: Christian de Muizon

In compliance with the *ICZN*, printed versions of all papers are deposited in the libraries of the institutes that are members of the *EJT* consortium: Muséum National d'Histoire Naturelle, Paris, France; National Botanic Garden of Belgium, Meise, Belgium; Royal Museum for Central Africa, Tervuren, Belgium; Natural History Museum, London, United Kingdom; Royal Belgian Institute of Natural Sciences, Brussels, Belgium; Natural History Museum of Denmark, Copenhagen, Denmark.